USING DENDROCHRONOLOGY AND ISOTOPE METHODS TO IDENTIFY THE WATERSHED ORIGIN OF WOOD IN THE RIVER CORRIDOR

by

SÁDE K. CROMRATIE CLEMONS

B.S., University of North Carolina at Chapel Hill, 2021

A thesis submitted to the

Faculty of the Graduate School of the

University of Colorado in partial fulfillment

of the requirement for the degree of

Master of Arts

Department of Geography

2023

Committee Members:

Holly R. Barnard

Katherine B. Lininger

J. Renée Brooks

Bradley Markle

Cromratie Clemons, Sáde K. (M.A., Geography)

Using Dendrochronology and Isotope Methods to Identify the Watershed Origin of Wood in the River Corridor

Thesis directed by Holly R. Barnard

ABSTRACT

Large wood (LW) is important to river corridors and can be recruited from hillslopes and valley bottoms. Identifying where LW comes from can be used to constrict wood budgets for rivers. There are few techniques to identify the source location of LW. I test new techniques for wood sourcing using dendrochronology and isotopes. This study was conducted in the West Creek watershed near Rocky Mountain National Park in Colorado, USA. I sampled from LW log jams (unknown species and *Picea engelmannii*) and standing trees (*Pinus ponderosa*, *Pseudotsuga menziesii*, and *Picea engelmannii*) of different hillslope positions (near-channel and upslope). I calculate basal area increment (BAI), ring width index (RWI), and $\delta^{18}O$ to test whether the source of LW could be identified based on the standing trees sampled. Using all three metrics (BAI, RWI, and $\delta^{18}O$), average time series and standing tree elevation correlations were used to describe trends in the data that could point to the source location of LW. I used significant difference testing to figure out whether the coefficient of variation (CV) or variance of each metric was different between positions and could be used to identify the source location of LW. I also used annual metric values to identify differences between positions based on drought conditions using Palmer Drought Severity Index (PDSI). T-tests were used to correlate annual metric values between LW and standing trees to see which hillslope position each LW piece correlated with the most. For all of my tests, there were only a few significant results. There were no differences in CV or variance for any of the species or metrics. Differences were

found between positions only for *Pinus ponderosa* BAI when including PDSI, but BAI was not different in all PDSI categories. *Picea engelmannii* showed both near-channel and upslope trees responded to climate, but in a similar way. Out of the small portion of t-test values that were considered significant, LW BAI was correlated most to the near-channel position. My results show that none of the metrics can be used with the tests chosen to identify the source location of LW. Addressing the limitations of this study is needed to determine whether dendrochronology and isotopes can be used to source the location of LW.

ACKNOWLEDGEMENTS

I would like to thank my advisor, Holly Barnard, and my co-advisor, Katherine Lininger, for guiding me through my program. I want to thank my other committee members, Renée Brooks and Bradley Markle, for helping with my thesis. Thank you to all the members of my lab groups for helping with field and lab work as well as defense preparation. I also would like to thank all the organizations that provided any funding that helped me present at conferences, pay for sample analysis, and support myself through my program. These organizations include: National Science Foundation (Award 2012669) Critical Zone Project, American Water Works Association Intermountain Section, Association for Women Geoscientist, Indian Peaks Wilderness Alliance, Institute of Arctic and Alpine Research (INSTAAR), and Inclusive Graduate Education Network (IGEN).

CONTENTS

TABLES

FIGURES

1. INTRODUCTION

Wood is an important component of river corridors (Jacobson et al., 1999; Piegay and Gurnell, 1997; Wondzell et al., 2009; Keys et al., 2018), defined as the channel, hyporheic zone, and floodplain (Harvey and Gooseff, 2015), because it influences many physical characteristics and ecological processes (Buffington et al., 2004; Wohl et al., 2019; Ruiz-Villanueva et al., 2019). Large wood (LW, diameter > 0.1 m, length > 1 m) impacts channel-floodplain connectivity and sediment transport and influences habitat diversity in and along rivers (Gurnell et al., 2002; Wohl et al., 2019; Keys et al., 2018; Gerhard and Reich, 2000). Large wood is also a relatively large organic carbon stock in forested river corridors, as approximately half of its mass is organic carbon (Scott & Wohl, 2020; Lininger et al., 2017; Russell et al., 2015). Understanding the source (e.g., hillslope versus riparian forest) and recruitment mechanisms of LW to the river corridor is fundamental to wood budgets that quantify inputs, outputs, and changes in LW storage (Benda et al., 2002; Wohl, 2017; Reid and Hassan, 2020; Lininger and Hilton, 2022). Wood budgets also provide a framework for understanding LW dynamics, carbon storage, and the impacts of disturbance and land management on LW abundance in streams (Benda et al., 2002; Reid and Hassan, 2020; Lininger and Hilton, 2022; Sutfin et al., 2016; Rathburn et al., 2017). However, the source of LW can be difficult to determine (Benda et al., 2002; Merten et al., 2013).

Large wood influences the structure of river corridors and is an important component of the wood regime, which is defined as the dynamic characteristics of recruitment, transport, and storage in rivers (Wohl et al., 2019). Mechanisms of LW recruitment include input from individual tree mortality and breakage, windstorms, wildfires, reintegration of LW previously buried in the stream bed and banks, transport from upstream, bank erosion, landslides,

avalanches, and debris flows from flooding (Benda et al., 2002; Wohl et al., 2019; Gurnell et al., 2002; Ruiz-Villanueva et al., 2019; Martin et al., 2023). Flooding impacts the wood regime by recruiting wood through mass movements on hillslopes and through erosion of the valley bottom (Piégay et al., 1999; Benda and Sias, 2003). Local LW inputs occurring near the stream are related mainly to bank erosion, while landslides can deliver LW from upslope (Benda et al., 2002; Reeves et al., 2003; Nakamura et al., 2000).

Multiple methods have been used to identify the spatial source of LW. Previous studies have attempted to determine the source location of LW using piece morphology (Benda et al., 2002; Reeves et al., 2003; Martin and Benda, 2001). For example, riparian inputs have been identified as relatively unbroken pieces with the root wad attached, whereas upslope LW inputs are more likely to have broken or abraded branches or be physically placed in or near landslide deposits (Benda et al., 2002; Reeves et al., 2003; Martin and Benda, 2001). Reeves et al. 's (2003) visual identification method assumed pieces sourced from the riparian zone were larger than pieces from upslope locations due to the breaking of hillslope-derived pieces during downslope travel. However, identifying the spatial source of LW from piece morphology can be inaccurate due to variations in piece morphology across source locations and the complexity of LW recruitment and transport. For example, root wads may or may not be present regardless of source location. Deposited pieces may be previously recruited and sourced from upstream bank erosion but have similar morphology to pieces subjected to hillslope transport and breakage (Reeves et al., 2003; McDade et al., 1990).

Other studies have tried to identify LW source using geomorphic context by assuming more LW pieces are recruited from hillslopes when the valley is narrow, hillslopes adjacent to channels are steep, or there are indications of hillslope failure (Benda et al., 2002; Reeves et al.,

2003). Identifying depositional locations also provides insight into possible LW source locations, characterizing trees connected to throw pits (soil depressions from uprooting) near the stream as riparian (Reeves et al., 2003). Limitations for this method arise because the source location of pieces may be easily identifiable if there is a clear indication of landslides or bank erosion near the deposited LW, but these methods are not a direct and precise approach of determining the source location of mobile wood pieces within a stream (Benda et al., 2002; Reeves et al., 2003).

Dendrochemistry has also been used to identify LW source locations. Specifically, metal concentrations within the wood have been used to track the source location of LW in tributaries at the sub-basin scale (Piégay et al., 2017). Riparian trees can take up metals in stream water and store those metals in their wood (Piégay et al., 2017; Sheppard, 1975; Yanosky and Vroblesky, 1992). Piégay et al. (2017) initially analyzed the metal concentrations of standing trees along tributaries subject to gravel mining to determine if it was possible to differentiate the signature by sub-basin. Using the metal concentrations of riparian trees and comparing them against the metal concentrations of in-stream wood deposited downstream in the mainstem of the Isère River in France, Piégay et al. (2017) identified the sub-basins from which the deposited wood was sourced. However, this method only works if the standing trees have a distinct dendrochemical signature that can be used to trace the LW back to its source location.

Another method involves the individual tagging of LW pieces to track pieces moving through the river network (Lininger and Hilton, 2022; Warren and Kraft, 2008; Hilton, 2012) which can be useful for determining if wood deposited within a reach came from upstream. Lininger and Hilton (2022) used repeat field surveys and tagging of downed pieces to identify input mechanisms for LW pieces and assess transport mobility through the stream. However, tagging individual LW pieces is time intensive and requires subsequent LW surveying of the

study site to assess changes over time. MacVicar et al. (2009) used radio frequency identification tags on standing trees within 5 meters of a frequently eroding bank to track lateral and downstream wood mobility and deposition in rivers. However, depending on the type of tags used, tracking wood using radio frequency tags can be expensive, and is subject to issues such as the inability to detect and find tags over longer distances (MacVicar et al., 2009).

Dendrochronology (the study of tree ring time series) techniques coupled with stable isotope composition ($^{18}O/^{16}O$) of wood cellulose may provide further insight into LW source location. Tree rings and stable isotopes are both used as proxies for changes in climate and are sensitive to local environmental conditions such as soil moisture (Depante et al., 2019; Rossatto et al., 2012; Li et al., 2007; Vysotskaya and Vaganov, 1989; Siegwolf et al., 2022). Soil moisture changes along hillslopes in semi-arid regions with soil moisture being lower upslope compared to near-channel positions due to the gravitational drainage of water downslope (Hosty and Mulqueen, 1996; Hewlett and Hibbert, 1963). Because tree growth is sensitive to soil moisture content (Teskey and Hinckley, 1986), trees growing in upslope locations tend to have less growth than those growing in near the stream during dry conditions (Li et al., 2007; Vysotskaya and Vaganov, 1989; Adams et al., 2014). Upslope trees could grow more or less than riparian trees based on soil moisture conditions and their stress tolerance (Rossatto et al., 2012; Marigo et al., 2000; Peterken and Mountford, 1996). Specifically, semi-arid environments have a stronger, more variable growth response to soil moisture than humid environments (Fritts, 1966; Manrique-Alba et al., 2017). Variations in soil moisture driven by evaporation also drive spatial differences in the $\delta^{18}O$ composition of source water for trees across the landscape (Depante et al., 2019; Rossatto et al., 2012; Allen et al., 2022), and these differences are transferred to the isotopic composition of the wood cellulose (Epstein et al., 1977; Sheshshayee et al., 2005;

DeNiro and Epstein, 1981; Burk and Stuiver, 1981; Song et al., 2022). Because variations in soil moisture change from the near-channel to the upslope, there may be higher variation in dendrochronological metrics or $\delta^{18}O$ composition in upslope trees compared to near-channel trees because they may have more consistent access to water.

Dendrochronology and isotope methods have been used to determine the regional provenance of wood and explain climate trends because correlations are expected to be stronger if the reference standing tree and the unknown wood grew in a similar climate (Haneca et al., 2005; Bernabei and Bontadi, 2011; Gut, 2018). These methods have identified the timber source for instruments, art, and buildings (Haneca et al., 2005; Bernabei and Bontadi, 2011; Sass-Klaassen et al., 2008; Bridge, 2012). However, research using dendrochronology and isotope methods to determine the provenance of LW recruited to river corridors has not been adequately explored. This research aims to combine dendrochronology methods with stable isotope methods to determine the source of LW (e.g., near-channel or hillslope) within a single catchment. The overarching goal is to determine if the differences between standing tree growth and $\delta^{18}O$ can be used to identify the source location of LW. Specifically, I ask:

1. Is the annual growth different between upslope and near-channel trees?
2. Do upslope trees have more variability in growth and $\delta^{18}O$ than near-channel trees?
3. Are upslope trees more enriched in $\delta^{18}O$ than near-channel trees?

2. OXYGEN ISOTOPE THEORY

Isotopes are atoms of the same element that differ in neutrons and have different atomic mass. The most common oxygen isotope found in nature is ^{16}O, but the heavier, less abundant ^{18}O is also found and has an additional two neutrons. The abundance of an isotope refers to the proportion of a particular isotope in a sample (Clark and Fritz, 1997; Milton and Wielgosz, 2002). The isotopic ratio describes the abundance of one isotope over the abundance of another, with the more abundant isotope being in the denominator (Urey, 1948; Milton and Wielgosz, 2002). Oxygen-16 is more abundant in nature, has a smaller atomic mass (isotopically light), and has weaker bonds, causing it to react faster than Oxygen-18 (isotopically heavy) during a reaction and move faster during diffusion (Clark and Fritz, 1997). The isotope ratio between Oxygen-18 and Oxygen-16 is written as $^{18}O/^{16}O$. To allow comparison across studies, isotope ratios are normalized relative to the isotope ratio of a common standard: expressing delta values (δ) in parts per thousand (‰) (Gonfiantini, 1984; Urey, 1948). The isotope ratio relative to the common standard is written as $\delta^{18}O$ and calculated using equation 1:

$$\delta^{18}O(‰) = \left(\frac{Rsample}{Rstandard} - 1\right) \times 1000 \qquad \text{Equation 1}$$

Changes in isotope ratios occur because of fractionation and mixing. Fractionation changes isotope abundance in the environment because of chemical and physical processes, causing an increase in one isotope relative to the other (Urey, 1947). In the following section, I review key processes that affect the isotope ratios found in wood cellulose to demonstrate why LW pieces may have different isotope ratios if sourced from different hillslope positions (e.g., valley bottom or riparian versus upslope).

Oxygen isotopes are often used as tracers that can help determine the source of water. The signal of $\delta^{18}O$ in tree ring cellulose can be traced back to the water source (Sargeant et al.,

2019; Penna et al., 2020) because the oxygen isotope signature in wood cellulose reflects changes in soil water isotopes from precipitation inputs and evaporation as well as changes in leaf water isotopes through transpiration, sucrose synthesis, and cellulose synthesis. The isotopic composition of water in the soil is related to the isotopic value of water infiltrating into and evaporating from the surface. The isotope signature of source water is affected by seasonal changes in precipitation. The isotope signature of summer precipitation is heavier than winter precipitation because of temperature differences during condensation and the source of water vapor (Beria et al., 2018). Before trees take up water, changes in the isotope signature of source water can also occur through evaporative enrichment and water-mixing in the subsurface during precipitation (Dawson, 1993; Dawson and Pate, 1996; Buhay and Edwards, 1995; Bigeleisen, 1962; Allen et al., 2022). The $^{18}O/^{16}O$ will increase within a pool of water as it evaporates (increasing $\delta^{18}O$) because ^{16}O will evaporate more readily than ^{18}O with mass-dependent fractionation (Dansgaard, 1954; Bigeleisen, 1962). The soil depth affects the oxygen isotope value, with shallow soils being more influenced by summer rain infiltration and evaporation both of which will increase $\delta^{18}O$ (Tang and Feng, 2001). In the Intermountain West, deep soil water is typically isotopically light (lower $\delta^{18}O$) because the primary source is snowmelt (Tang and Feng, 2001; Gazis and Feng, 2004; Caldwell, 1985; Harvey, 2005; Chimner and Cooper, 2004). Deep soil layers are also not exposed to as much evaporation as shallow soil layers, resulting in less evaporative enrichment in $\delta^{18}O$ for deep soil layers (Zimmermann et al., 1968; Gazis and Feng, 2004). Enrichment and depletion of ^{18}O in $\delta^{18}O$ values is relative to the system, so the magnitude of isotopic enrichment in soil water is based on the proportion of water that has evaporated, and the proportion of summer versus winter precipitation (Allen et al., 2022).

After soil water enrichment, the source water from the soil is taken up through the xylem.

For most trees, isotope fractionation or discrimination generally does not occur during the transport of water from the soil to the root, xylem, and stem (Dawson and Ehleringer, 1991; Wershaw et al., 1966). Although some studies have shown oxygen isotope fractionation during root water uptake in both drought-sensitive and drought-tolerant species (Poca et al., 2019; Vargas, 2017; Vega-Grau, 2021), no studies have looked at this type of fractionation in the species I sampled (*Pinus ponderosa*, *Pseudotsuga menziesii*, and *Picea engelmannii*). Therefore, the isotope composition is assumed to stay the same from the point of uptake until it reaches the leaf. Once the water reaches the leaves, fractionation occurs because of evaporation through transpiration (Dongman et al., 1974; Saurer et al., 1998; Wershaw et al., 1966).

Both transpiration and stomatal conductance change because of soil moisture and vapor pressure deficit (VPD), which is the difference between actual moisture in the air and the amount of moisture the air can hold at a given temperature. Higher soil moisture allows the stomata to open more compared to lower soil moisture, resulting in higher stomatal conductance and transpiration (Lange et al., 1971; Meinzer, 1993; Bond et al., 2008). In dry soil conditions, the stomata will close to reduce transpiration and conserve water (Lange et al., 1971). Stomatal conductance and transpiration are also responsive to VPD of the air. Stomatal conductance increases in moist air (Tuzet et al., 2003), but a decrease in VPD drives a decrease in transpiration. Oxygen isotopes are related to transpiration in a similar way as evaporation. Initially, high ^{18}O can be seen at the site of evaporation in leaves when they transpire because the light isotopes (^{16}O) are evaporating faster, leaving more ^{18}O (Sheshshayee et al., 2005; Farquhar and Lloyd, 1993).

The isotope difference between source water and leaf water at the site of evaporation (the substomatal cavity within the leaf) is described using the Craig-Gordon equation (Craig and

Gordon, 1965; Dongmann et al., 1974; Farquhar and Lloyd, 1993):

$$\Delta^{18}O_e = \varepsilon^+ + \varepsilon^k + (\Delta^{18}O_v - \varepsilon^k)\left(\frac{e_a}{e_i}\right) \quad \text{Equation 2}$$

where $\Delta^{18}Oe$ is the evaporative enrichment of leaf water at the site of evaporation, ε^+ and ε^k are the equilibrium fractionation factor and kinetic fractionation factor respectively, $\Delta^{18}O_v$ is the isotopic composition of atmospheric water vapor relative to the source water, and $\frac{e_a}{e_i}$ is defined as the ratio of water vapor pressure in the air (e_a) to the water vapor pressure internal to the leaf (e_i) (Craig and Gordon, 1965; Dongmann et al., 1974; Farquhar and Lloyd, 1993). The $\Delta^{18}Oe$ is dependent on $\frac{e_a}{e_i}$ and the fractionation factors. The $\frac{e_a}{e_i}$ regulates atmospheric vapor exchange with leaf water: at high $\frac{e_a}{e_i}$ atmospheric vapor which is isotopically depleted in ^{18}O exchanges readily with leaf water, whereas at low $\frac{e_a}{e_i}$ the exchange is limited, causing leaf water at the site of evaporation to be more enriched in ^{18}O.

Leaf water at the site of evaporation is more enriched than bulk leaf water (Equation 3) and is dependent on how much isotopically enriched water back diffuses into the bulk leaf. High transpiration limits back-diffusion of this enriched water to the chloroplasts where sugars are formed (Barbour, 2007), and is described in the following equation:

$$\Delta^{18}O_L = \Delta^{18}O_e\left(\frac{1-e^{-\wp}}{\wp}\right) \quad \text{Equation 3}$$

where $\Delta^{18}O_L$ represents the enrichment of bulk leaf water relative to source water and $\wp$ represents the Péclet number (Barbour, 2007; Farquhar and Lloyd, 1993; Barbour and Farquhar, 2000). When transpiration is high, the back-diffusion of enriched water is reduced since the flux of unenriched water is equivalent to the transpiration rate. This causes an inverse relationship between enrichment and transpiration and stomatal conductance known as the Péclet effect (Equation 4). The Péclet number is calculated using the equation below:

$$\wp = \frac{EL}{CD} \qquad \text{Equation 4}$$

where L represents the effective path length in the leaf, E is the transpiration rate, C is the molar concentration of water, and D is the diffusivity of $H_2{}^{18}O$ in water (Farquhar and Lloyd, 1993; Cuntz et al., 2007). Holding everything else constant, increasing the transpiration rate will increase the Péclet effect and will result in a lower contribution of enriched water to the $\delta^{18}O$ of bulk leaf water which represents the water where sugars are formed and ultimately the leaf water signal that is incorporated into cellulose.

Additional biochemical fractionation occurs during sugar development from photosynthesis (Equation 5) (Farquhar and Lloyd 1993; Gessler et al., 2014; Roden et al., 2000). The isotope difference between sucrose and source water is calculated as:

$$\Delta^{18}O_{suc} = 1.027\Delta^{18}O_L + 27‰ \qquad \text{Equation 5}$$

where $\Delta^{18}O_{suc}$ is the isotopic enrichment of sucrose relative to source water, $\Delta^{18}O_L$ is the isotopic enrichment of bulk leaf water (Barbour et al., 2007; Cernusak et al., 2003). The sugars are either stored as starch (no fractionation from starch creation) or moved to other parts of the plant as sucrose (Roden et al., 2000). As sucrose travels through the phloem, oxygens on sucrose may exchange with xylem water (Gessler et al., 2014; Roden et al., 2000). When sucrose is then broken down to create cellulose, some oxygen contained in sucrose exchanges with xylem water (Sternberg et al. 2006; Sternberg and DeNiro, 1983; Barbour, 2007), and additional fractionations occur. The resulting cellulose is more isotopically enriched in ^{18}O (higher $\delta^{18}O$ values) than leaf water and sucrose (Equation 6) (Sternberg and DeNiro, 1983; Roden et al., 2000). The enrichment of cellulose is represented by the equation:

$$\Delta^{18}O_{cel} = \Delta^{18}O_L(1 - p_{ex}p_x) + \varepsilon_{wc} \qquad \text{Equation 6}$$

where p_{ex} is the proportion of exchangeable oxygen found in cellulose during formation, p_x is the proportion of unenriched xylem water found during cellulose formation in the cell walls, and ε_{wc} is the equilibrium fractionation factor of oxygen in water and carbonyl groups (Barbour and Farquhar, 2000).

As a result of these combined processes, cellulose $\delta^{18}O$ can vary by landscape position because of source water, relative humidity ($\frac{e_a}{e_i}$), and transpiration differences. Soil moisture conditions tend to be drier upslope compared to lower slope positions because of an increase in evaporation in upper soil layers and gravitational drainage in deeper soil layers (Hosty and Mulqueen, 1996; Cooper et al., 1990; Hewlett and Hibbert, 1963), causing changes in $\delta^{18}O$ by position (Depante et al., 2019; Rossatto et al., 2012; Nippert and Knapp, 2007). If the transpiration rate, relative humidity, and Péclet number are held constant between all positions, $\delta^{18}O$ composition in tree ring cellulose will be affected mostly by source water.

If trees in the upslope position take up water in topmost, drier soil layers, they will be more enriched in ^{18}O (from $\delta^{18}O$) than near-channel trees because of soil evaporation. Most roots in ponderosa pine, Engelmann spruce, and Douglas-fir are in the upper 60 cm soil (Burns, 1990), so I expect differences in $\delta^{18}O$ between upslope and near-channel trees because of the evaporative enrichment of the upper soil layers. However, if soil moisture is consistent along a hillslope and precipitation is frequent, the $\delta^{18}O$ signal could be similar for all positions due to the mixing of newly precipitated water with old soil water that is more depleted in ^{18}O (lower $\delta^{18}O$ values).

3. METHODS

3.1 Study Site

I conducted my study in the West Creek watershed (N 40° 26.6', W 105° 27.9'), located in the semi-arid Rocky Mountains of Colorado, USA (Figure 1). West Creek drains southeast from Rocky Mountain National Park and into the North Fork Big Thompson River and has an elevation of 2200 m to 3552 m and a drainage area of 59 km². Annual precipitation totals and annual mean temperature range from 311 mm to 676 mm and 5°C to 8°C over a 61-year (1960-2021) period, respectively (https://prism.oregonstate.edu/explorer/). River discharge in the watershed increases in the late spring and early summer due to snowmelt, as well as in response to convective storms in the summer (Sibold et al., 2006). In 2013, an extreme precipitation event occurred along the Colorado Front Range with rainfall totals over 450 mm (Gochis et al., 2015). West Creek watershed is located in the Colorado Front Range and was affected by the flood, with rainfall totals between 177.9 and 228.6 mm and a peak discharge with an estimated 400-yr recurrence interval (~311.5 m^3s^{-1}) (Yochum and Moore, 2013; Gochis et al., 2015).

Due to the 2013 flood, erosion occurred along the floodplain and on the hillslopes of West Creek, causing LW recruitment and deposition to the river corridor. (Lininger et al., 2021; Guiney and Lininger, 2022). The West Creek valley bottom contains a large amount of LW stored in jams relative to floodplains not impacted by the 2013 flood, with the average jam load and jam size being 678.59 m^3 ha^{-1} and 9.78 m^3, respectively (Lininger et al., 2021). The valley bottom is closely connected to the hillslopes due to a relatively narrow valley in some river reaches, thus the sources of LW in the existing jams deposited during the 2013 flood is likely from hillslope as well as valley bottom inputs from floodplain erosion (Guiney and Lininger, 2022). I sampled from two West Creek reaches (reach 28 and reach 34), with the naming

convention taken from Guiney and Lininger (2022) indicating the distance (in 100-m increments) upstream of the confluence with the North Fork Big Thompson River. I selected both reaches because of their different hillslope and bank erosion characteristics. Within reach 28 (the downstream reach), a small hillslope failure is visible on the river right bank (Figure 1), while the hillslope within reach 34 remained stable during the 2013 flood (the upstream reach). With a hillslope failure present in reach 28 and absent in reach 34, the mechanism for introducing LW into the channel could differ between reaches, but downed LW pieces within both reaches could have come from valley bottom erosion or hillslope failures.

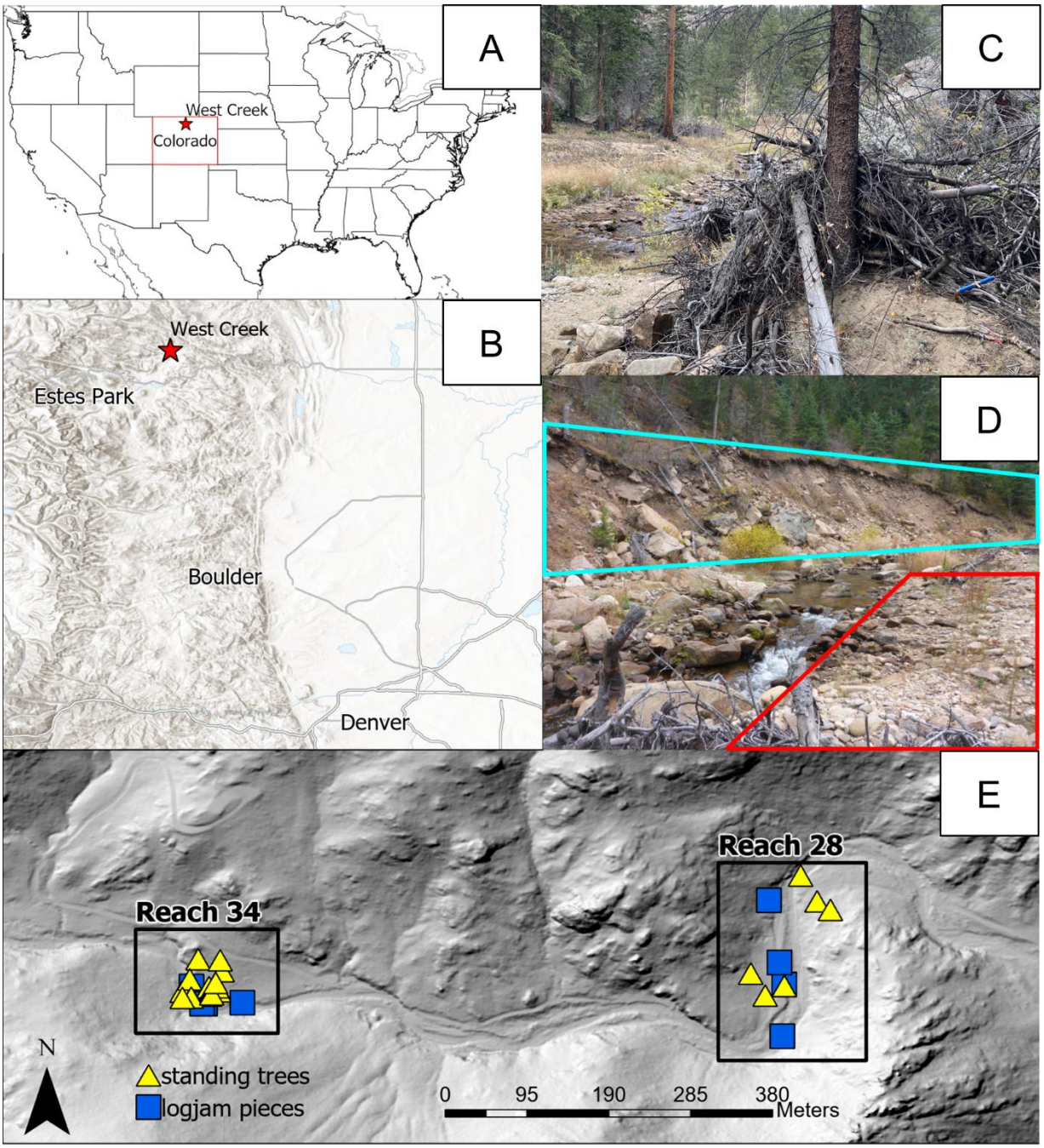

Figure 1. Study site location indicated with a star in the contiguous United States (A) and in Colorado (B). Reach 34, showing a logjam (C). Reach 28, showing a hillslope failure (blue box) and scoured bank and floodplain (red box) (D). Hillshade map of study reaches with locations of sampled standing trees and logjam pieces (E).

3.2 Tree Ring Sampling and Measurements

In October 2021, I collected tree cores using a 12 mm diameter increment borer. I sampled from common upper montane zone tree species present in the study area, including

Pinus ponderosa (ponderosa pine), *Pseudotsuga menziesii* (Douglas-fir), and *Picea engelmannii* (Engelmann spruce). The diameter at 1.4 m (breast height) was recorded for all living trees sampled. I collected LW disks and pieces (¼ of a full disk) from LW jams (n = 10) using a hand saw and recorded the diameter of each LW piece at the point of sampling. The vertical distance and horizontal distance of each tree and LW sample from the bankfull stream channel edge to the tree breast height were recorded using a TruPulse laser rangefinder and corrected to get the distance from the channel to the base of the tree (Table 1, Appendix Table A1). After field sampling, I used the elevation above the channel (vertical distance between the stream channel edge and the base of the sampled tree) to categorize the tree samples into near-channel and upslope positions. Two samples in the upslope position were not recorded using the TruPulse laser rangefinder, so I used GPS points and a 1m Digital Elevation Model (DEM) to determine the distance of the tree from above the channel. The upslope position was identified as any tree greater than 2 m in elevation above the channel, while near-channel was anything less than or equal to 2 m. The coordinates of each sample were recorded using GaiaGPS (Version 1.1, 2021). I took standing tree cores (n = 21) at different landscape positions (near-channel and upslope) to capture variability in standing tree samples across potential source locations. At reach 28, I sampled ponderosa pine (n = 3) and Engelmann spruce (n = 3) at both near-channel and upslope positions (total n = 6 cores). At reach 34, I took samples from ponderosa pine (n = 6), Engelmann spruce (n = 6), and Douglas-fir (n = 3) at near-channel and upslope positions (total n = 15 cores).

Table 1. Standing tree data including species, reach, hillslope position, and tree elevation difference from stream (vertical distance). Ponderosa pine (Pipo), Douglas-fir (Psme), Engelmann spruce (Pien).

Tree ID	Species	Reach	Position	Elevation from Stream (m)
Standing 1	Pien	28	Near-Channel	-0.4
Standing 2	Pien	28	Upslope	2.4
Standing 3	Pien	28	Upslope	5.7
Standing 4	Pipo	28	Near-Channel	1.2
Standing 5	Pipo	28	Upslope	2.7
Standing 6	Pipo	28	Upslope	6
Standing 7	Pien	34	Near-Channel	0.7
Standing 8	Pien	34	Near-Channel	0.8
Standing 9	Pien	34	Near-Channel	1.3
Standing 10	Pien	34	Near-Channel	2
Standing 11	Pien	34	Upslope	2.5
Standing 12	Pien	34	Upslope	3
Standing 13	Pipo	34	Near-Channel	1.3
Standing 14	Pipo	34	Near-Channel	1.3
Standing 15	Pipo	34	Upslope	2.5

Tree ID	Species	Reach	Position	Elevation from Stream (m)
Standing 16	Pipo	34	Upslope	2.6
Standing 17	Pipo	34	Upslope	7.2
Standing 18	Pipo	34	Upslope	6.5
Standing 19	Psme	34	Near-Channel	1.6
Standing 20	Psme	34	Upslope	2.6
Standing 21	Psme	34	Upslope	7

3.3 Tree Ring Sample Processing and Isotope Analysis

The tree cores were air-dried and sanded until the earlywood-latewood boundaries could be clearly identified visually. Tree rings were scanned using an Epson Expression 10000 XL digital scanner (Regent Instruments, Quebec, Canada) and measured using WinDENDRO software (Regent Instruments, Quebec, Canada). Cores were scanned at 2400 dpi and measured at an accuracy of 0.001 mm. I checked the cores for false rings, and marker years (2002, 2006, 2012) indicating drought conditions were used to cross-date. LW disks were measured using sections of the disks that had the best ring visibility.

To compare growth differences among landscape positions, I calculated basal area increment (BAI) from raw ring widths and tree diameters and ring width index (RWI) from raw ring widths using the dlpR package in R (Bunn et al., 2022). Basal area increment (Equation 7) is a measure of radial growth and is calculated by taking the total basal area of the current year minus the basal area of the previous year (Hornbeck and Smith, 1985):

$$BAI = \pi r_t^2 - \pi r_{t-1}^2 \qquad \text{Equation 7}$$

where *r* is tree radius and *t* is the current tree ring year.

I calculated the RWI by dividing the raw ring width of each annual growth increment by the predicted value for a given growth increment based on the spline curve fit for each tree's time series (Cook and Peters, 1981). A 2/3 cubic smoothing spline with 50% frequency was used to detrend the ring widths and remove age-growth-related trends (Cook and Peters, 1981). Using a cubic smoothing removes low-frequency variability, including age-related trends, while preserving high-frequency climate variability (Cook and Peters, 1981; Cook, 1985). The resulting detrended data was used for statistical analysis.

To prepare the tree rings for cellulose extraction to determine the isotopic composition, I separated the tree rings by year and finely ground them using a ball mill (Retsch MM 400). When the rings were too small to use the ball mill because too much mass would be lost to processing, I finely chopped them by hand using razor blades. Each tree ring was extracted to produce alpha-cellulose, a structural component of wood, following the methods of Leavitt and Danzer (1993).

The $\delta^{18}O$ values of cellulose were measured at the Stable Isotope Facility at the University of Wyoming. The analysis was run using a temperature conversion elemental analyzer (TC/EA, ThermoScientific, Massachusetts, United States) for pyrolysis and an isotope ratio mass spectrometer (IRMS, Thermo Delta Plus, Massachusetts, United States) for analysis of the resultant gas. The isotope ratios of the tree rings were calibrated and assessed for quality control using the University of Wyoming's internal reference standards for organic material.

International standards IAEA 601 and IAEA 602 (both benzoic acid) were used to calibrate the quality control and quality assurance lab standards. Isotope values were corrected

using linear normalization and the ratios were referenced to the Vienna Standard Mean Ocean Water (VSMOW) standard (Equation 1). Samples were analyzed in a total of 3 analytical sets, with each set including two calibration standards for normalization, and one quality assurance standard. A total of 17 sample duplicates were ran with the 3 analytical sets. Quality assessment and control measures were taken to calculate lab accuracy and precision, which were recorded as -0.27 ‰ and 0.34 ‰, respectively. Sample precision based on the 17 duplicates was recorded as 0.46 ‰.

3.4 Climate and Meteorology Data

To determine the tree growth response to annual climate conditions, I acquired Palmer Drought Severity Index (PDSI) data for the time period 1960-2021 for Colorado Platte Drainage division (54,159.34 km^2) from the National Climate Data Center (http://www.ncdc.noaa.gov/cdo-web/). The Palmer Drought Severity Index is a measure of meteorological drought based on a water balance model including local precipitation and temperature indices (Palmer 1965, Heddinghaus and Sabol, 1991). I used five classes of PDSI to classify water availability and moisture conditions of different years across the growing season (May-September). Based on classifications described in Palmer (1965) and Heim (2002), the PDSI classification I used included: extreme drought (values -4.00 and below), severe drought (values -3.99 to -3.00), moderate drought (values -2.99 to -2.00), mid-range (values -1.99 to 1.99), moderately moist (values 2.00 to 2.99), very moist (values 3.00 to 3.99), and extremely moist (values 4.00 and above).

3.5 Descriptive Statistics

To quantify time-series trends between positions, percent change in BAI was calculated for each position of each species. I also calculated percent change between drought years and

non-drought years to compare percent change between positions. For the RWI and $\delta^{18}O$ time series, minimum and maximum values were highlighted to show the range of RWI and $\delta^{18}O$ between positions. The RWI and $\delta^{18}O$ for each drought year were identified to show tree response to stress by position. For LW, I used samples of high growth and low growth to compare BAI ranges and drought year growth by position. I used ranges and standard deviations to identify LW that had high and low variation in RWI and $\delta^{18}O$. I identified the RWI and $\delta^{18}O$ in drought years to show the responsiveness of LW to climate.

3.6 Data Analysis

Statistical analysis was done in R (Version 2022.07.1) (R Core Team, 2022). No statistical test was used for Douglas-fir due to low sample size (n =1 for near-channel, n = 2 for upslope). I used Spearman correlation coefficients to identify relationships between BAI coefficient of variation (CV), $\delta^{18}O$ variance, and RWI variance and elevation difference. Variance is the spread of values in a data set and CV is the distribution of values around the mean, but both are a measure of variability. To determine if there is a relationship between tree growth and landscape position, I calculated the variance of the RWI and $\delta^{18}O$ and CV of the BAI for each standing tree time series (each tree core calculated independently). The coefficient of variation is only calculated for BAI in order to standardize the values and show relative variability around the mean. I tested differences in these metrics using Kruskal-Wallis and Mann–Whitney U tests to determine if each metric varied by landscape position within each species. Due to the relatively small sample size, I compared the results to an alpha level of 0.05 and 0.1.

To assess the relationship between growth response to climate, I created boxplots for each species comparing PDSI and growth (BAI and RWI) at each position. I also used Kruskal-

Wallis (Pairwise Wilcoxon as post-hoc test) and Mann–Whitney U tests to determine significant differences among growth and positions in PDSI-classified drought conditions. I also did the same statistical analysis on $\delta^{18}O$ values to further assess climate's role on tree rings at different positions.

Drawing on dendroprovenancing techniques used for identifying wood origin, I used tree series correlations to best identify the source location of the LW. I used standing trees as reference tree ring series, correlating them with the LW series (Figure 2). Because of the low sample size, I calculated the Spearman correlation coefficients (ρ) of BAI and RWI between standing tree records and LW records. Using the correlation coefficient, I calculated t-values (Equation 8) in R:

$$t = \rho\sqrt{\frac{N-2}{1-\rho^2}} \qquad \text{Equation 8,}$$

where N is the number of years the reference series and logjam series have in common, ρ is Spearman's correlation coefficient, and t is the test statistic (Baillie, 2014; Gut, 2018; Leland et al., 2021). High t-values between the LW and reference trees are assumed to indicate the best position match out of all tree rings used for comparison (Baillie, 2014). A limitation of this method is the required length of a time series for the results to be accurate. Many studies have used a minimum of 50-100 years (Baillie, 2014; Boswijk and Fowler, 2019; Hanca et al., 2005; Bernabei and Bontadi, 2011); however, Sass-Klaassen et al. (2008) successfully provenanced wood using a minimum series of 41 years. In my dataset, the length of the time series varied between all three metrics. Reference time series for $\delta^{18}O$ were limited to years 2005 to 2013, while longer time series were created for RWI and BAI for standing trees (1999-2013). The shortest and longest time series from the unknown LW samples was from 1999 to 2013 and 1984 to 2013, respectively. It should be noted that because of the short length of each time series and

the short length of overlap, the accuracy of matching the LW with the standing trees is reduced. Studies that used Spearman correlation coefficients, which have a more flexible sample size requirement than traditional Pearson correlation, still used an overlap length greater than 50 years (Gut, 2018; Martin-Benito et al., 2014). However, Weigl (2006) states that a minimum of 30 years of overlap is required to use t-values. Based on the smallest overlap that could be found in the literature, only LW that had an overlap of at least 30 years was used to calculate t-values.

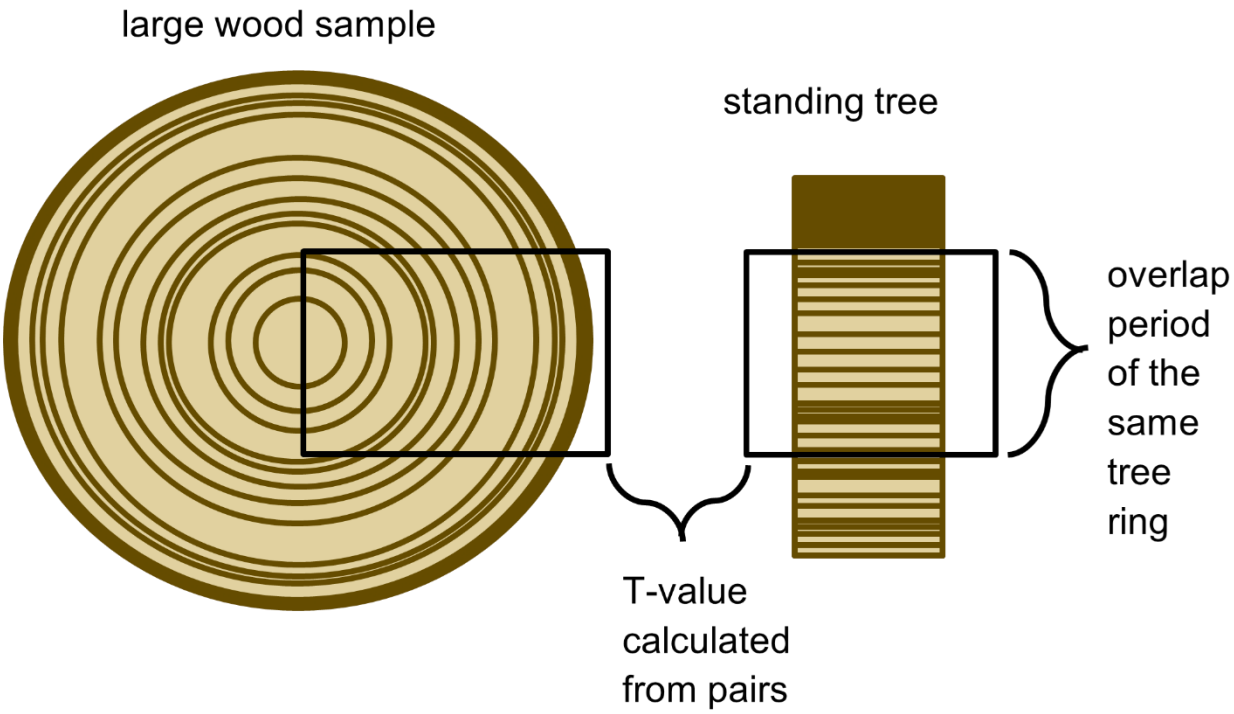

Figure 2. T-value matching using unknown large wood piece and standing tree core.

4. RESULTS

4.1 Growth Trends Through Time for BAI and RWI and $\delta^{18}O$

Over a full time-series, upslope trees were expected to have lower growth than near-channel trees because of water limitations for upslope trees. Based on descriptive statistics, upslope trees grew less than near-channel trees for all species (Figure 3 a-c). For ponderosa pine, the average BAI for the full time series period (1999-2013) was 35.48% lower in upslope trees (mean = 863.60 mm², standard error (SE) = 36.02 mm²) compared to near-channel trees (mean = 1338.46 mm², SE = 86.53 mm²) (Figure 3a). The average BAI also was 33.7 % lower in upslope Engelmann spruce trees (mean = 1401.72mm², SE= 95.78 mm²) compared to near-channel trees (mean = 2113.77 mm², SE = 89.15 mm²) (Figure 3b). There was only one near-channel Douglas-fir used to calculate the average BAI for the full time series. There was little difference between the upslope and near-channel Douglas-fir trees, with BAI being 12.7 % less in upslope trees (mean = 860 mm², SE = 95.84 mm²) than the near-channel tree (mean = 985.32 mm², SE = 103.17 mm²) (Figure 3c). Accounting for the sample size of Douglas-fir (n = 3), the percent change in average BAI is small between positions compared to ponderosa pine and Engelmann spruce. The trend of a smaller average BAI in upslope trees can be used to describe subtle growth differences between positions.

The average BAI and standard error values were calculated for each position during the drought years 2002, 2006, 2012 and compared against the average BAI in non-drought years to see if isolating drought years showed greater growth differences than looking at time series averages that fluctuate between dry and wet years. All species decreased in average BAI during drought years compared to non-drought years, but upslope trees had a greater decrease in average drought year BAI than near-channel trees. The average ponderosa pine BAI was 24.14%

lower in upslope trees (688.32 mm², SE = 15.78 mm²) and 13.90% lower in near-channel trees (1185.38 mm², SE = 151.75 mm²) during drought years compared to non-drought years (Figure 3a). For Engelmann spruce, the average BAI was lower during drought years for both upslope (923.30 mm², SE = 88.37 mm²) and near-channel (1682.21 mm², SE = 229.92 mm²) trees by 39.31% and 24.28 % respectively (Figure 3b). Upslope Douglas-fir's average BAI (336.79 mm², SE = 72.30 mm²) was 66.01% lower in drought years than non-drought years, while the near-channel tree's average BAI (723.26 mm², SE = 201.12 mm²) was 31.17% lower in drought years (Figure 3c). Looking at response to climate during drought years between positions may prove to be a more reliable indicator of hillslope position than average growth across an entire time series.

The RWI emphasizes a tree's growth variation relative to climate so RWI measurements can indicate a change in growth response between hillslope position. Ponderosa pine had a similar RWI range in upslope trees (range = 1.74, 0.27 - 2.01) and near-channel trees (range = 1.74, 0.29 - 2.03) (Appendix Figure A1). However, the RWI range was larger in upslope Engelmann spruce trees (range = 1.55, 0.26 - 1.81) than near-channel trees (range = 1.23, 0.23 - 1.46) (Appendix Figure A2). The upslope and near-channel Douglas-fir follow a similar trend as ponderosa pine with a similar range in upslope trees (range = 1.67, 0.25 - 1.92) and near-channel trees (range = 1.69, 0.50 - 2.19) (Appendix Figure A3). Engelmann spruce showed the largest variation in RWI range between positions, which suggests that upslope Engelmann spruce follows expectations and may have greater variance than near-channel trees.

Examining RWI for each drought year could give more insight on responsiveness to drought for both near-channel and upslope trees, which could be used to differentiate between positions. When comparing the average RWI of multiple trees between positions during drought years, upslope trees are not always lower than near-channel trees in average RWI. The average

RWI for upslope ponderosa pine is slightly lower than near-channel ponderosa pine in 2002 (upslope = 0.83, near-channel = 0.86), lower in 2006 (upslope = 0.84, near-channel = 1.18), and higher in 2012 (upslope = 0.88, near-channel = 0.67) (Figure 3d). For Engelmann spruce, average upslope RWI was lower in 2002 (upslope = 0.52, near-channel = 0.71), slightly lower in 2006 (upslope = 0.51, near-channel = 0.56), and higher in 2012 (upslope = 0.63, near-channel = 0.56) (Figure 3e). Upslope Douglas-fir had a similar RWI to near-channel trees during 2002 (upslope = 0.51, near-channel = 0.50), lower RWI in 2006 (upslope = 0.25, near-channel = 0.51), and lower RWI in 2012 (upslope = 0.32, near-channel = 1.22) (Figure 3f). Douglas-fir responded as expected, with upslope RWI being generally lower than near-channel trees during drought years (Figure 3f). Because the near-channel RWI was not consistently higher than upslope RWI for all species, using descriptive statistics for average RWI during drought years may not be a reliable indicator of hillslope position.

I found that upslope trees met the expectation that they would have greater range of $\delta^{18}O$ in comparison to near-channel trees for one of the species. The $\delta^{18}O$ range was 26.6 ‰ to 36.9 ‰ for the full-time series for all species. For ponderosa pine (Appendix Figure A4), upslope trees had higher minimum and maximum $\delta^{18}O$ values than near-channel trees, but the upslope $\delta^{18}O$ range (range = 6.03, 29.6 ‰ - 35.6 ‰) was similar to the near-channel $\delta^{18}O$ range (range = 6.2, 27.4 ‰ - 33.6 ‰). Engelmann spruce had a greater $\delta^{18}O$ range in upslope trees (range = 9.93, 27.0 ‰ - 36.9 ‰) than near-channel trees (range = 7.1, 26.6 ‰ - 33.7 ‰) (Appendix Figure A5). Upslope Douglas-fir (range = 3.41, 28.7 ‰ - 32.1 ‰) had a similar $\delta^{18}O$ range to near-channel trees (range = 2.45, 28.7 ‰ - 31.1 ‰) (Appendix Figure A6). I only observed differences in Engelmann spruce, so $\delta^{18}O$ ranges may not be a good indicator of ecophysiological responsiveness to soil moisture between positions.

During drought conditions, the $\delta^{18}O$ was expected to be greater in upslope trees because there is more enrichment from soil water evaporation. The $\delta^{18}O$ for each drought year tended to be higher than for non-drought years for both upslope and near-channel trees, but the species responded differently with respect to position. For ponderosa pine, the $\delta^{18}O$ during drought years were similar in both 2006 (upslope = 32.5 ‰, near-channel = 32.4 ‰) and 2012 (upslope = 32.2 ‰, near-channel = 31.6 ‰) when considering sample precision (± 0.46 ‰) (Figure 3g). Upslope Engelmann spruce had a higher $\delta^{18}O$ than near-channel trees during both 2006 (upslope = 32.7 ‰, near-channel = 31.0 ‰) and 2012 (upslope = 32.8 ‰, near-channel = 30.3 ‰) (Figure 3h). Upslope Douglas-fir had a slightly higher $\delta^{18}O$ than near-channel Douglas-fir during 2006 (upslope = 31.1 ‰, near-channel = 30.0 ‰), but both positions had a similar $\delta^{18}O$ during 2012 (upslope = 30.7 ‰, near-channel = 31.0 ‰) (Figure 3i). My results indicate that using $\delta^{18}O$ values from drought years without additional testing is not a reliable hillslope position indicator.

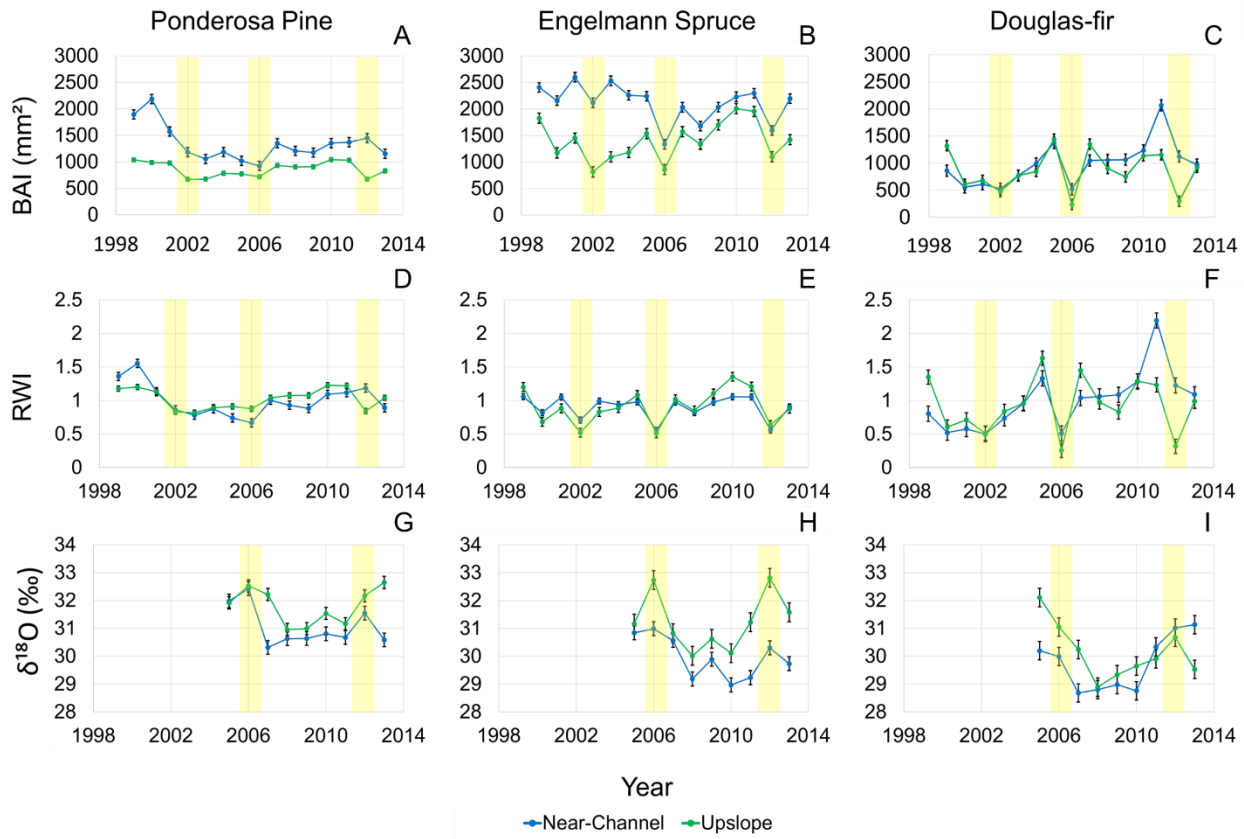

Figure 3. Time series plots with average basal area increment (BAI), ring width index (RWI), and $\delta^{18}O$ of standing trees for ponderosa pine, Engelmann spruce, and Douglas-fir. Shaded yellow region indicates drought years.

To examine how LW incremental growth trends related to those of the live standing trees, I examined the LW samples that appeared to be the most and least responsive to climate conditions and also the LW samples that could be identified as Engelmann spruce. Of the unknown LW samples, LW-9 had the lowest range in BAI (range = 319.29, 666.58 mm² - 347.29 mm²) and LW-6 had the greatest range in BAI (range = 1905.24, 3082.89 mm² - 1177.64 mm²) (Figure 4a, Appendix Table A2). The Engelmann spruce samples were identified as LW-5 (range = 955.67, 393.13 mm² - 1348.80 mm²) and LW-2 (range = 309.66, 352.90 mm² - 662.56 mm²) (Figure 4d, Appendix Table A2).

LW samples were compared against standing trees based on percent changes in average BAI during drought years (2002, 2006, 2012) and non-drought years to see if the LW responds

similarly to near-channel or upslope trees. Both unknown LW samples decreased in average BAI during drought years, but LW-6 had a greater decrease in average BAI which indicates a greater response to drought than LW-9 (Figure 4a). LW-6, the sample with the highest growth response, had a 28.99 % decrease in average BAI during drought years (1602.58 ± 358.53 mm²) compared to non-drought years (2257 ± 115.61 mm²) (Figure 4a). However, it is hard to tell which position LW-6 could have possibly come from because its response to drought years is similar to upslope trees and near-channel trees. LW-9, the sample with the lowest growth response, had 6.02 % decrease in average BAI during drought years (527.72 ± 50.30 mm²) compared to non-drought years (561.51 ± 28.54 mm²) (Figure 4a). When comparing against the average drought year BAI for near-channel and upslope trees, LW-9 responded similarly to near-channel trees of all species and had a small percent change between drought years and non-drought years, so LW-9 could come from near the channel. The Engelmann spruce sample, LW-5, decreased in average BAI by 8.52 % between drought years (812.19 ± 189.38 mm²) and non-drought years (812.19 ± 189.38 mm²) (Figure 4d). LW-2 had a 21.25 % decrease in average BAI during drought years (432.53 ± 35.88 mm²) compared to non-drought years (549.24 ± 30.86 mm²) (Figure 4d). LW-2 had a greater response to drought than LW-5, but both LW-2 and LW-5 have small percent changes similar to that of near-channel trees. Additional statistical tests are needed for identifying source location.

I report trends in the unknown and Engelmann spruce LW samples with the greatest and least variation in RWI over the timeseries to identify similarities between LW and standing trees. LW-4, the unknown LW sample with the largest variation in RWI had a range of 1.41 (0.56-1.97) (Figure 4b, Appendix Table A2). LW-3 had the lowest RWI variation in unknown LW, with a range of 0.34 (0.77 - 1.12) (Figure 4b, Appendix Table A2). For Engelmann spruce LW,

LW-5 had a range of 0.44 (0.72 - 1.17), while LW-2 had a range of 0.52 (0.68 - 1.20) (Figure 4e, Appendix Table A2).

The average RWI during each drought year was calculated for each LW sample and compared against the average RWI for both near-channel and upslope trees to see if the LW had similar RWI values to near-channel or upslope trees. The RWI response to drought years varied by LW sample, but LW-4 and LW-3 had opposite responses to drought years (Figure 4b). LW-4 responded to drought years with a decrease in relative growth during 2002 (0.72), increase in 2006 (1.13), and another decrease in 2012 (0.67) compared to non-drought years. LW-4 had similar drought year values to average near-channel and upslope time series (Figure 4b, Appendix Table A3). LW-3 had a similar RWI to non-drought years in 2002 (1.01), slightly decreased in 2006 (0.90), and slightly increased RWI in 2012 (1.10) (Figure 4b, Appendix Table A3). Similar to LW-4, the drought years of LW-3 varied and did not follow a specific near-channel or upslope trend. For Engelmann spruce LW, LW-2 decreased in RWI during 2002 (0.86), 2006 (0.68), and 2012 (0.88) compared to non-drought years of the same time series (Figure 4e, Appendix Table A3). There was also no pattern for LW-2. LW-5 decreased in RWI during 2002 (0.72) and slightly decreased during 2006 (0.94) and 2012 (0.95) compared to non-drought years (Figure 4e, Appendix Table A3). LW-5 also was not similar to a specific position. Comparing the drought year RWI for LW against the average drought year RWI time series values does not indicate where the wood comes from.

I identified unknown LW samples that had the largest variation in $\delta^{18}O$ and Engelmann spruce LW based on their range. The $\delta^{18}O$ range for unknown and Engelmann spruce LW was similar to the range found in standing trees. Out of all the unknown LW, LW- 1 was the sample with the smallest variation in $\delta^{18}O$ and had a range of 1.88 (29.0 ‰ - 30.8 ‰) (Figure 4c,

Appendix Table A2). LW-7 had the highest variation in $\delta^{18}O$ and had a range of 5.64 (31.0 ‰ - 36.6 ‰) (Figure 4c, Appendix Table A2). For Engelmann spruce LW, LW-2 had the largest variation and a range of 3.42 (29.1 ‰ - 32.5 ‰), while LW-5 had the lowest variation and a range of 2.25 (32.3 ‰ - 34.5 ‰) (Figure 4f, Appendix Table A2).

Similar to RWI, I used the unknown and Engelmann spruce LW average $\delta^{18}O$ during drought years to compare against the near-channel and upslope trees to identify similarities in average $\delta^{18}O$ values. The $\delta^{18}O$ response varied during drought years in my LW samples. Unknown species LW-7 had a $\delta^{18}O$ of 36.6 ‰ during 2006 and 32.9 ‰ during 2012, which is higher compared to most of the non-drought years on the time-series (Figure 4c, Appendix Table A3). LW-7 is the most similar to upslope Engelmann spruce in terms of drought years. LW-1 had higher $\delta^{18}O$ during 2006 (30.3 ‰) and 2012 (30.8 ‰) compared to non-drought years (Figure 4c, Appendix Table A3). LW-1 had drought years that were the most similar to near-channel Douglas-fir. For Engelmann spruce LW, LW-2 had higher $\delta^{18}O$ during 2006 (30.6 ‰) and 2012 (31.3 ‰) than at least half of the non-drought years (Figure 4f, Appendix Table A3). The drought year $\delta^{18}O$ was the most similar to that of near-channel Engelmann spruce. LW-5 increased in $\delta^{18}O$ for both drought years (2006 = 33.8 ‰, 2012 = 34.5 ‰) compared to non-drought years and was similar in drought years to upslope Engelmann spruce (Figure 4f, Appendix Table A3). Most of the LW samples described were similar in near-channel and upslope Engelmann spruce $\delta^{18}O$ during drought years specifically, which was the only species that previously showed varying $\delta^{18}O$ between positions (Figure 3h). However, statistical analysis needs to be done to figure out if differences in $\delta^{18}O$ are present between positions to find out where LW comes from.

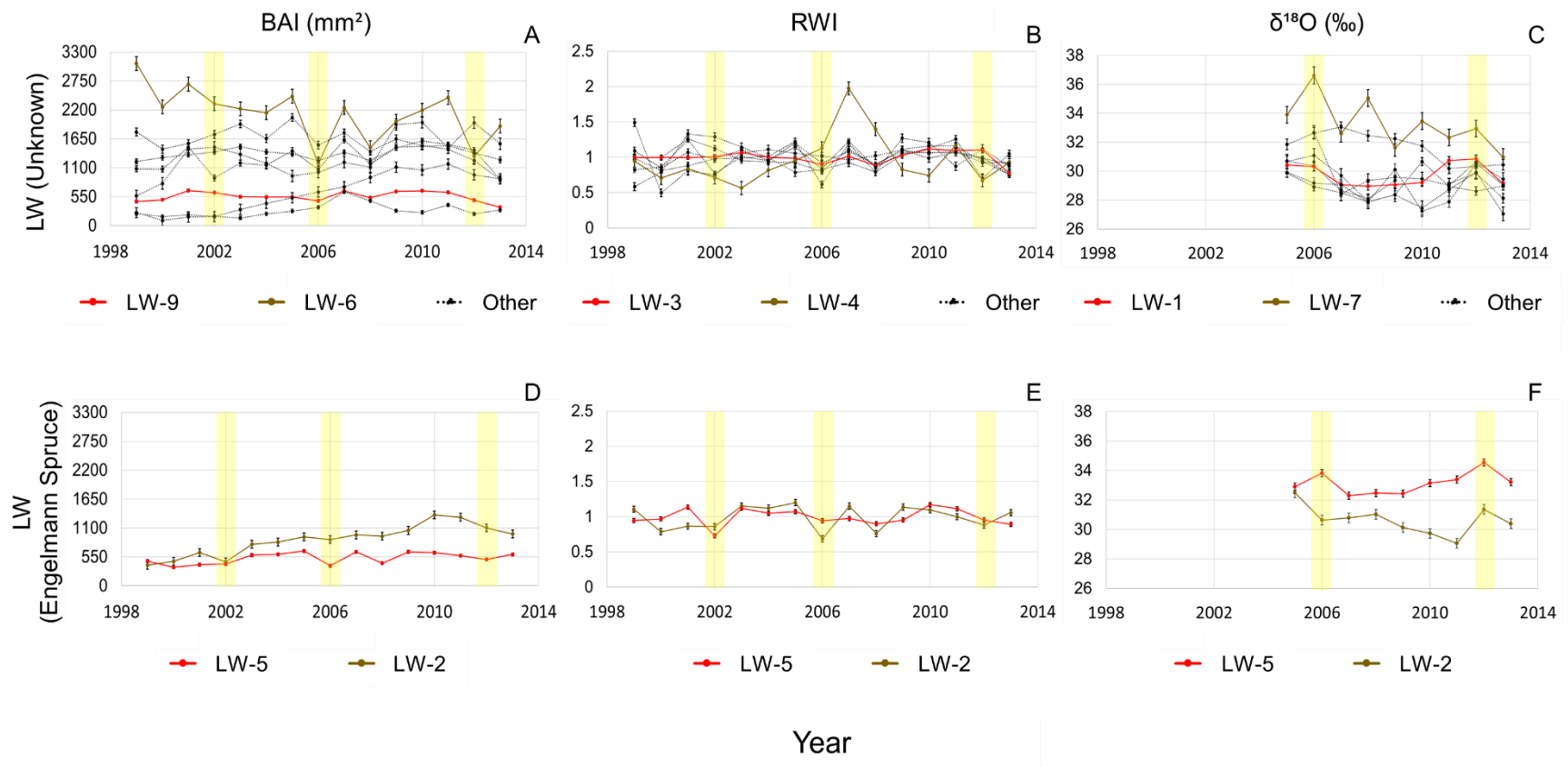

Figure 4. Time series plots with basal area increment (BAI), ring width index (RWI), and $\delta^{18}O$ for large wood of known species (LW Engelmann spruce) (D-F) and unknown species (LW Unknown) (A-C). Shaded yellow region indicates drought years.

4.2 BAI and RWI and $\delta^{18}O$ variability by elevation difference

It was expected that elevation above the channel would show a positive relationship with BAI CV, RWI variance, $\delta^{18}O$ variance, because the variability in growth and isotope signature would increase for trees farther from the channel based on differences in evaporation. No significant ponderosa pine correlations were found for $\delta^{18}O$ variance, BAI CV, or RWI variance in relation to elevation above the channel, with Spearman's correlation coefficients of -0.04 ($p = 0.91$), -0.08 ($p = 0.83$), and -0.23 ($p = 0.54$), respectively (Figure 5a). For Engelmann spruce, elevation above the channel was correlated with BAI CV ($\rho = 0.73$, $p = 0.03$), but not $\delta^{18}O$ variance ($\rho = 0.03$, $p = 0.95$) or RWI variance ($\rho = 0.58$, $p = 0.11$) (Figure 5b). Correlation coefficients were not calculated for Douglas-fir because of a low sample size ($n = 3$). No correlations were significant, except for BAI CV for Engelmann spruce, indicating the variation in my measured tree ring attributes are not a good indicator of hillslope position.

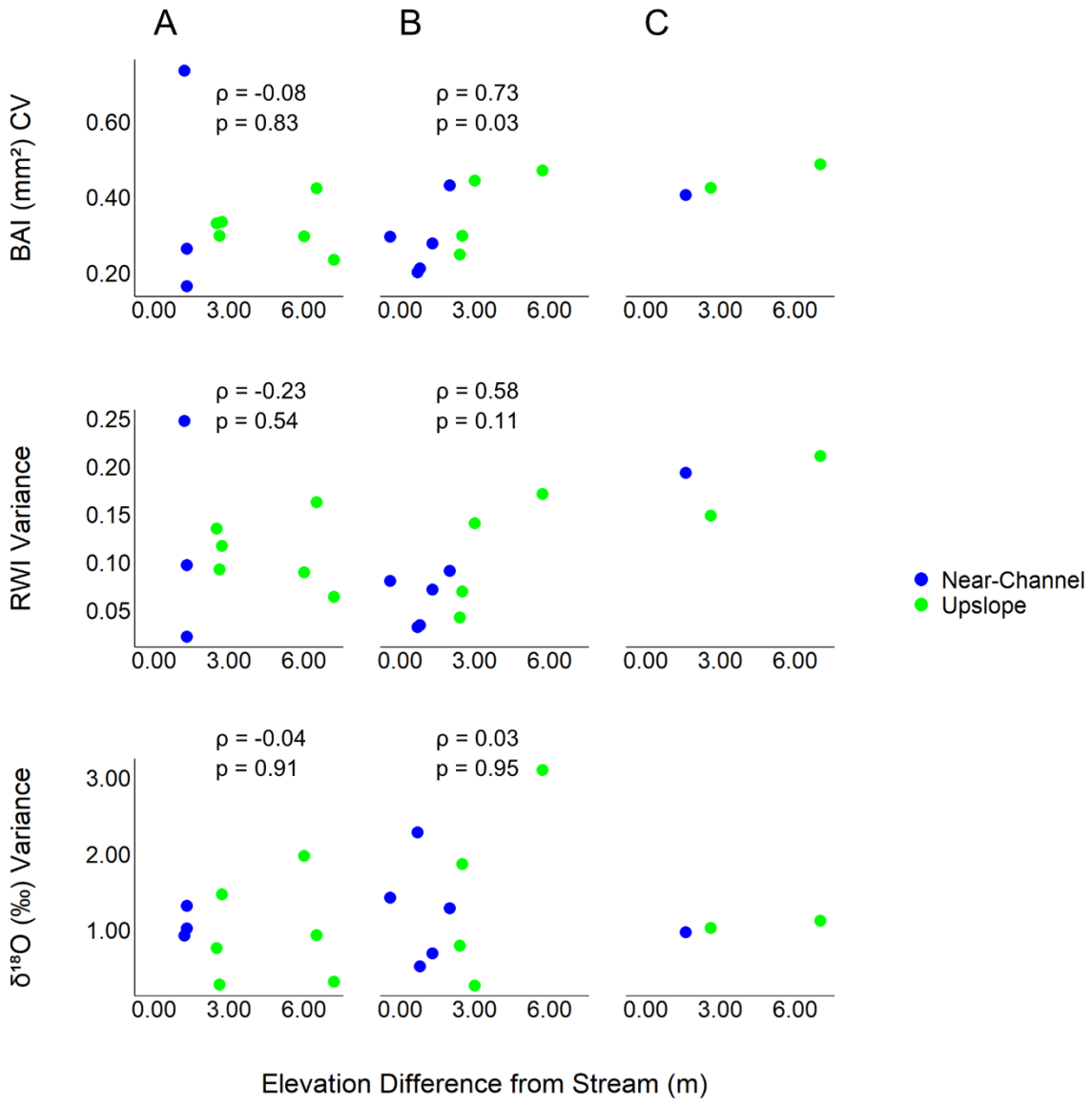

Figure 5. Scatter plots showing basal area increment (BAI) coefficient of variation (CV), ring width index (RWI) variance, and $\delta^{18}O$ variance across elevation for (A) ponderosa pine, (B) Engelmann spruce, and (C) Douglas-fir. Correlation coefficient (ρ) and p-value (p) are displayed.

4.3 Comparison of BAI and RWI Variability by Landscape Position and Species

With the assumption that upslope trees have more stress during drought conditions, I expected growth variability to be different between positions, with upslope trees having more growth variability than near-channel trees. I tested for differences between positions for each species to determine if near-channel and upslope trees differed in growth through time. No

differences in BAI CV were found between positions for ponderosa pine ($p = 0.71$) or Engelmann spruce ($p = 0.19$) (Figure 6a,b). The unknown LW and Engelmann spruce LW overlapped both landscape positions for ponderosa pine and Engelmann spruce as well as upslope trees for Douglas-fir (Figure 6a-c). There were not enough differences between positions to infer where the LW pieces came from.

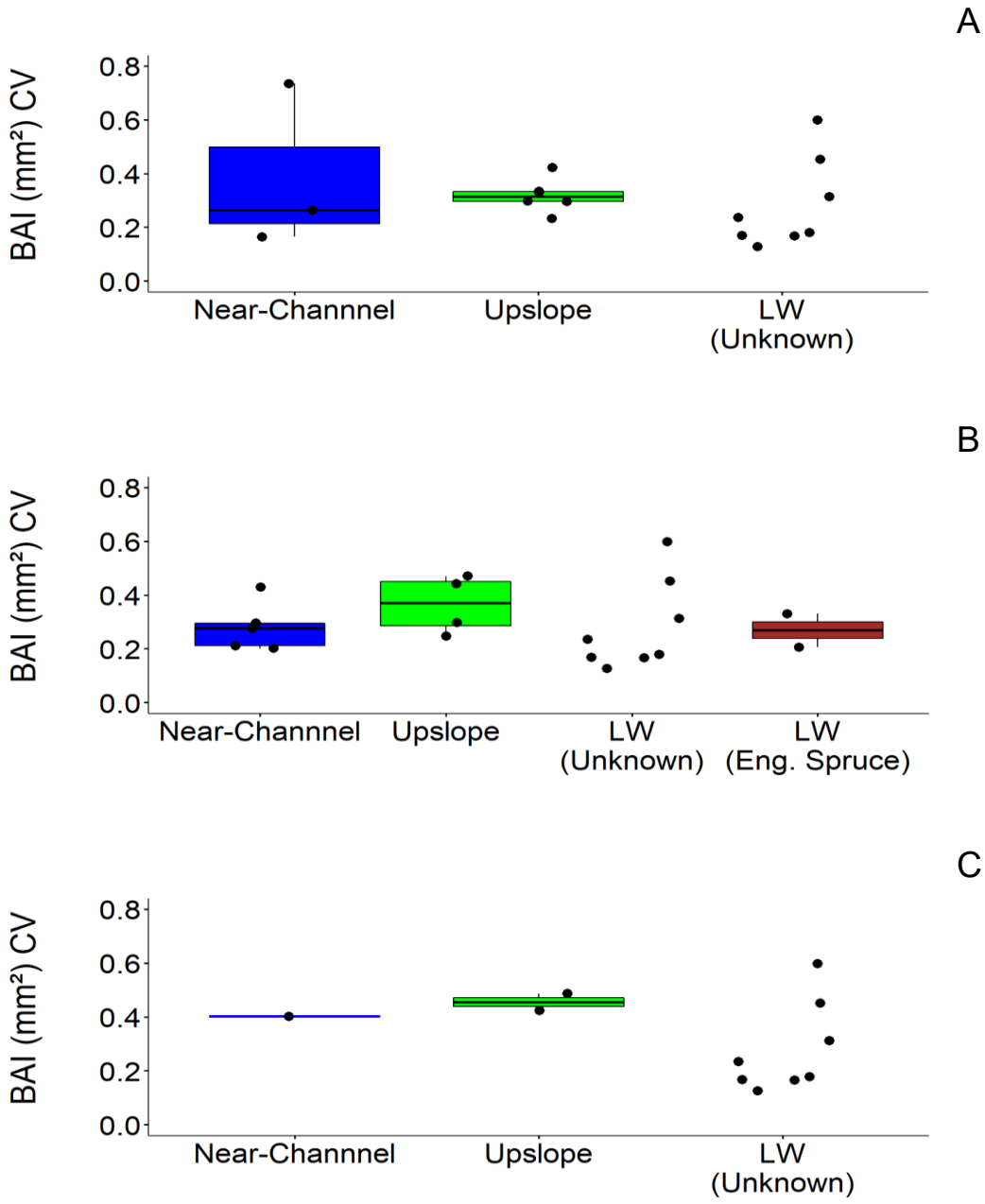

Figure 6. Boxplots of basal area increment (BAI) coefficient of variation (CV) by position for (A) ponderosa pine, (B) Engelmann spruce, (C) Douglas-fir. Jitter points show the BAI CV of each standing tree and large wood (LW) sample. LW is separated between Engelmann spruce and unknown species.

Similar to BAI CV, I expected RWI variance to be more variable in upslope trees because of sensitivity to water conditions. The results of Mann–Whitney U showed no significant difference in RWI variance between positions for ponderosa pine ($p = 1.00$) or Engelmann spruce

(p = 0.41) (Figure 7a,b). The RWI variance of unknown LW and Engelmann spruce LW overlapped with both positions for all species (Figure 7a-c). There were no differences in variance between positions to identify the source location of LW.

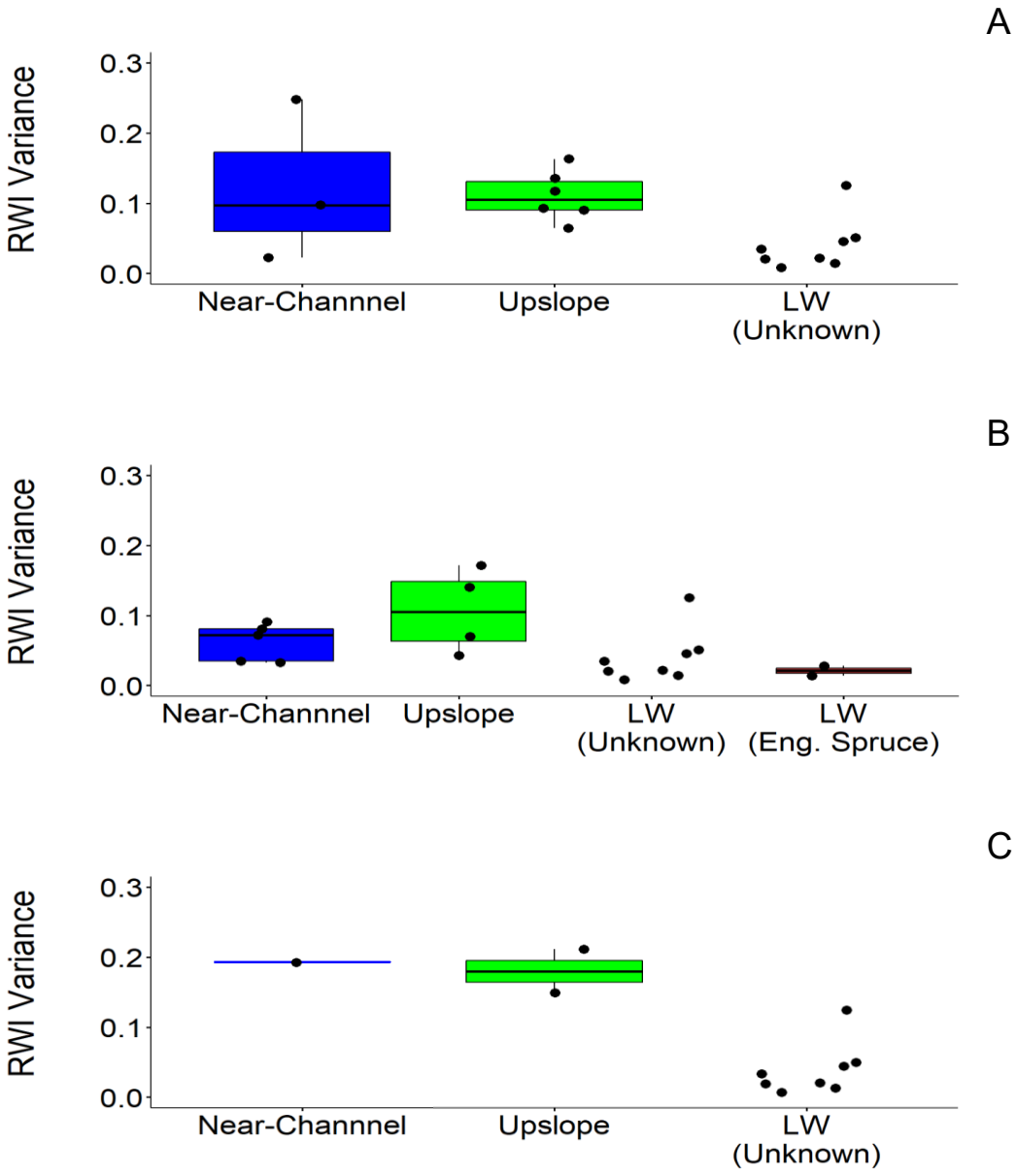

Figure 7. Boxplots of ring width index (RWI) variance by position for (A) ponderosa pine, (B) Engelmann spruce, (C) Douglas-fir. Jitter points show the RWI variance of each standing tree and LW sample. Large wood (LW) is separated between Engelmann spruce and unknown species.

4.4 Comparison of BAI and RWI by Landscape Position with Regard to Climate/PDSI

Because tree growth responds to climate conditions, I expected both upslope trees and near-channel trees to respond to PDSI with the possibility of both positions reacting differently to the same PDSI categories because of higher soil moisture for near-channel trees and lower soil moisture for upslope trees. Annual BAI was used to test differences across PDSI categories for near-channel and upslope trees separately to see if near-channel and upslope BAI responded to regional climate in a different way, with upslope trees responding more negatively to drought PDSI categories. The extremely moist drought category did not occur in the selected years (1999-2013) for analyses of BAI or RWI. The results of Kruskal-Wallis test showed no significant difference in upslope BAI ($p = 0.17$) or near-channel BAI ($p = 0.35$) across six PDSI categories for ponderosa pine, indicating that ponderosa pine growth does not vary considerably between years with different PDSI categories (Figure 8a). Although Kruskal Wallis calculated a marginal significant difference for upslope Engelmann spruce across PDSI categories ($p = 0.06$), there were no significant differences in upslope BAI found across PDSI groups during post-hoc comparison ($p > 0.24$ for all comparisons among categories) (Figure 8b). For near-channel Engelmann spruce, there was no significant difference in near-channel BAI across PDSI categories ($p = 0.27$) (Figure 8b). No differences were found for near-channel Douglas-fir, but the median BAI for upslope Douglas-fir was different between mid-range and extreme drought conditions ($p = 0.04$, mid-range = 920.9 mm^2, extreme drought = 386.89 mm^2) (Figure 8c, Appendix Figure A7). When separated by position, there were not enough evidence to suggest that BAI reacts differently to regional climate and cannot be used to identify growth differences for near-channel and upslope trees.

If local soil moisture was the main driver of tree growth, upslope BAI was expected to be different from near-channel BAI, specifically during dry conditions, with upslope BAI being lower

because of less local access to water. Within the PDSI categories, differences in annual BAI between positions were calculated to see differences in BAI during each PDSI category. The median BAI was lower in upslope ponderosa pine trees during extreme drought ($p < 0.01$, upslope = 738.7 mm^2, near-channel = 1293.96 mm^2), moderate drought ($p < 0.01$, upslope = 842.72 mm^2, near-channel = 1448.7 mm^2), mid-range ($p = 0.01$, upslope = 811.95 mm^2, near-channel = 1214.15 mm^2), and very moist conditions ($p = 0.05$, upslope = 985.07 mm^2, near-channel = 1828.74 mm^2) (Figure 8a, Appendix Figure A8). There were no significant differences in Engelmann spruce BAI ($p > 0.45$) or Douglas-fir BAI ($p > 0.26$) between near-channel and upslope trees when comparing within PDSI categories (Figure 8b,c). Although ponderosa pine was significantly different between positions, it was not for severe drought and moderately moist categories (Appendix Figure A8).

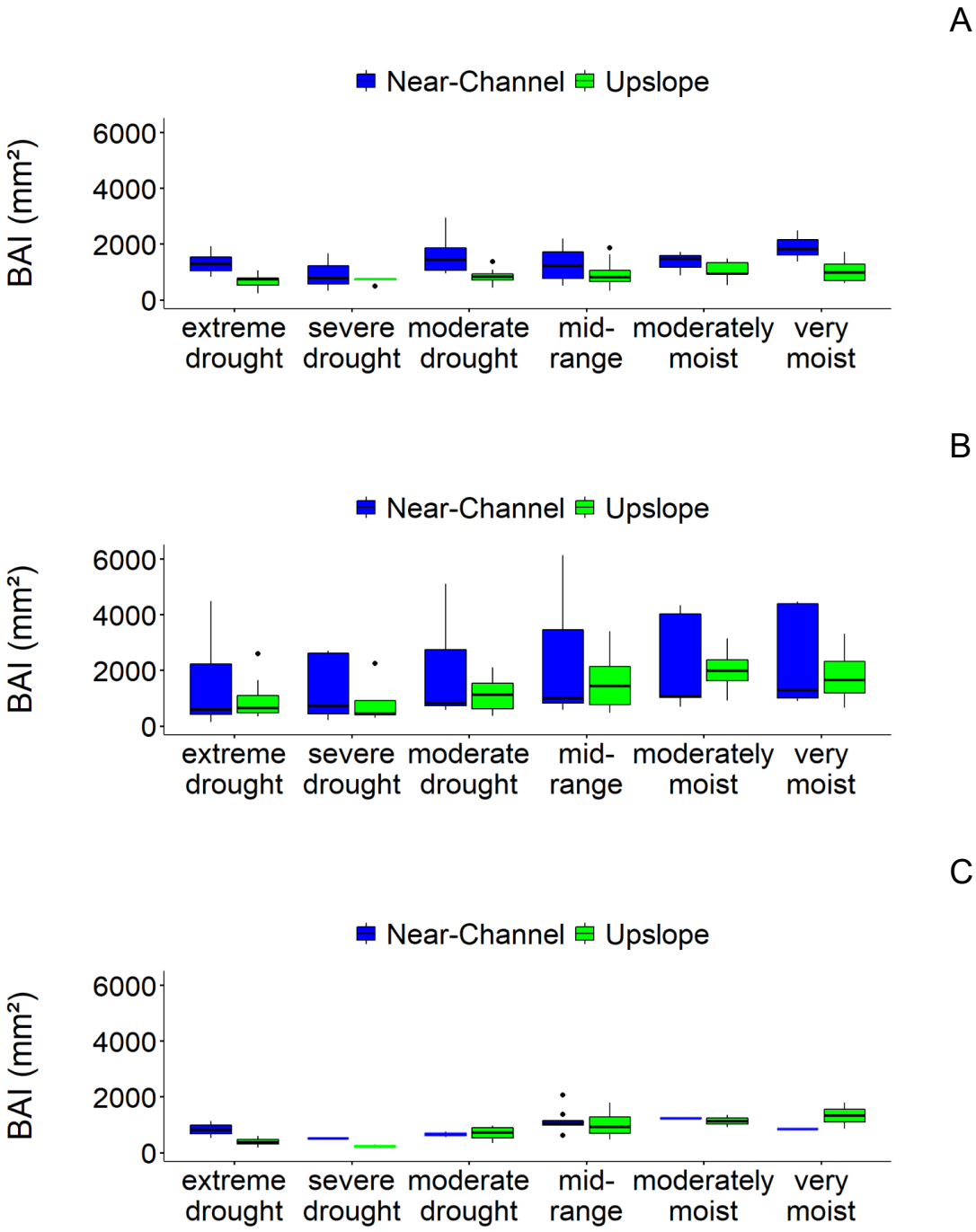

Figure 8. Boxplots of basal area increment (BAI) by position and PDSI category for (A) ponderosa pine, (B) Engelmann spruce, (C) Douglas-fir.

Both near-channel and upslope RWI for trees were expected to react to PDSI data because trees can vary in RWI in response to regional climate conditions. Annual RWI was used to test

differences across PDSI categories to see if near-channel and upslope RWI reacted differently to regional climate. No differences in RWI were found for near-channel ($p > 0.64$) or upslope ($p > 0.18$) ponderosa pine trees across PDSI drought categories (Figure 9a). In contrast the Engelmann spruce RWI shows a clear dependance on PDSI categories, with higher RWI under increasingly moist conditions. Differences were found in upslope Engelmann spruce RWI between extreme drought and mid-range ($p < 0.01$, extreme drought = 0.62, mid-range = 0.99), extreme drought and moderately moist ($p = 0.02$, extreme drought = 0.62, moderately moist = 1.25), and extreme drought and very moist ($p = 0.02$, extreme drought = 0.62, very moist = 1.18) (Figure 9b, Appendix Figure A9). Upslope Engelmann spruce also had differences in RWI between mid-range and moderate drought ($p = 0.03$, mid-range = 0.99, moderate drought = 0.73), mid-range and moderately moist ($p = 0.03$, mid-range = 0.99, moderately moist = 1.25), and mid-range and severe drought ($p = 0.02$, mid-range = 0.99, severe drought = 0.42) (Figure 9b, Appendix Figure A9). There were other differences in upslope Engelmann spruce RWI during moderately moist and moderate drought ($p = 0.02$, moderately moist = 1.25, moderate drought = 0.73) as well as moderately moist and severe drought ($p = 0.05$, moderately moist = 1.25, severe drought = 0.42) (Figure 9b, Appendix Figure A9). The RWI for upslope Engelmann spruce generally increased with increasing PDSI.

Differences were also found in near-channel Engelmann spruce RWI across PDSI categories. When comparing Engelmann spruce near-channel RWI during extreme drought to all other the PDSI categories, differences were found between extreme drought and mid-range ($p < 0.01$, extreme drought = 0.57, mid-range = 0.96), extreme drought and moderate drought ($p = 0.03$, extreme drought = 0.57, moderate drought = 0.89), extreme drought and moderately moist ($p = 0.04$, extreme drought = 0.57, moderately moist = 1.05), and extreme drought and very moist ($p =$

0.03, extreme drought = 0.57, very moist = 1.03) (Figure 9b, Appendix Figure A10). Differences in near-channel Engelmann spruce RWI were also found between severe drought and mid-range ($p < 0.01$, severe drought = 0.53, mid-range = 0.96), severe drought and moderate drought ($p = 0.03$, severe drought = 0.53, moderate drought = 0.89), severe drought and moderately moist ($p = 0.03$, severe drought = 0.53, moderately moist = 1.05), and severe drought and very moist ($p = 0.03$, severe drought = 0.53, very moist = 1.03). (Figure 9b, Appendix Figure A10). These results suggest that near-channel Engelmann spruce significantly reduced in growth under stressed conditions (severe drought and extreme drought) compared to other moist conditions, with a higher RWI in wetter conditions than drier conditions. Although differences were found for near-channel RWI and upslope RWI separately, they both react similarly across PDSI categories with higher RWI during wetter conditions (Appendix Figure A9, A10). A difference in RWI was also found for upslope Douglas-fir, but only between mid-range and extreme drought conditions ($p = 0.01$, mid-range = 1.05, extreme drought = 0.42) (Figure 9c, Appendix Figure A11). Looking at differences in RWI for near-channel and upslope trees has shown that trees, specifically Engelmann spruce, are reacting to regional climate regardless of landscape position.

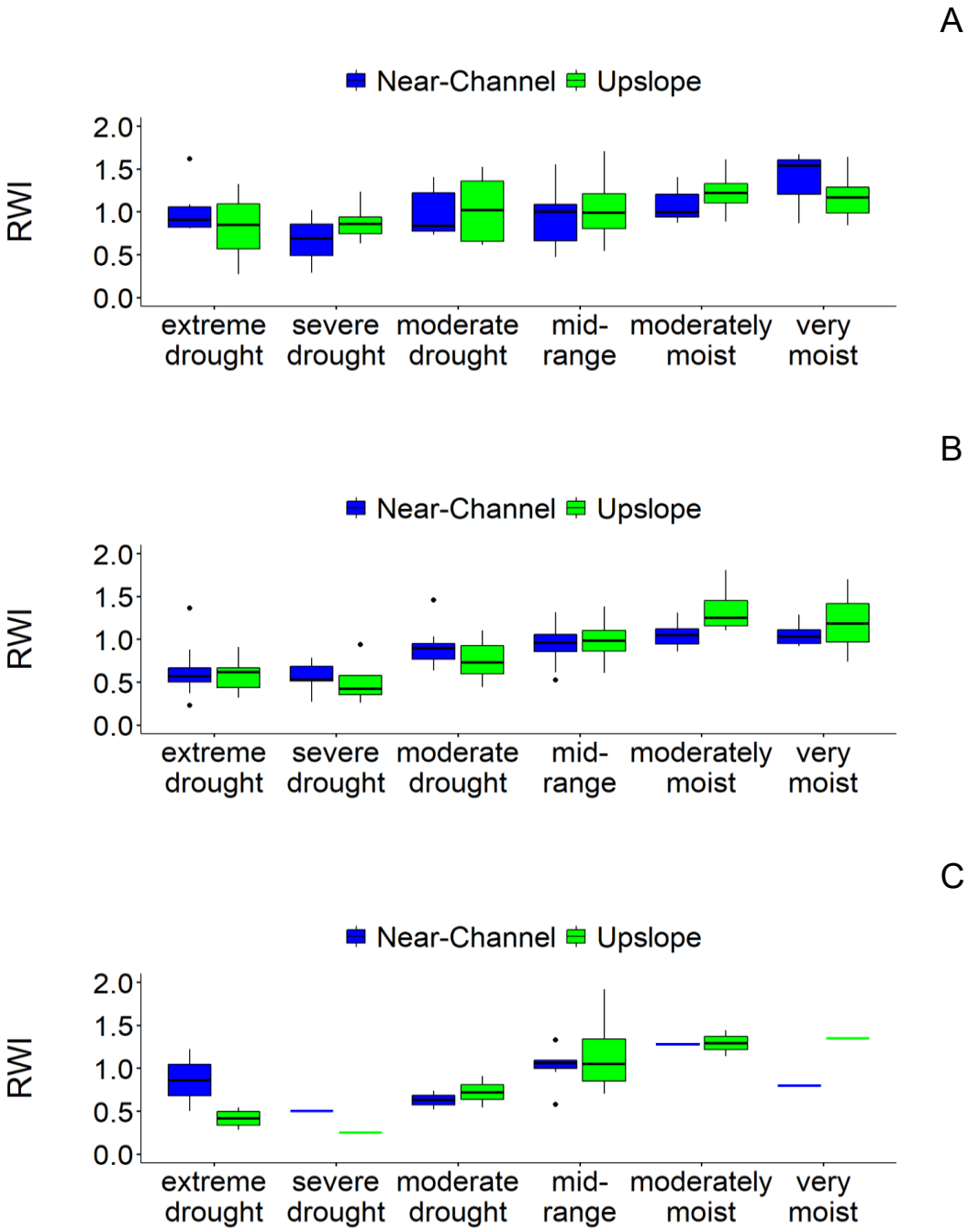

Figure 9. Boxplots of ring width index (RWI) by position and PDSI category for (A) ponderosa pine, (B) Engelmann spruce, (C) Douglas-fir.

4.5 T-value matching for BAI and RWI

Trees have yearly changes in growth and comparing growth from year to year between LW pieces could show how well the LW compares to near-channel or upslope trees, assuming year to

year growth is not the same for both positions. Spearman's correlation coefficients between all possible pairs of standing trees and LW samples were calculated using both BAI and RWI values to identify which position the LW sampled correlated with the most. The correlation coefficients ranged from 0.27 to 0.81 for BAI and from 0.39 to 0.85 for RWI (Appendix Table A4, A5). Because t-value matching requires a minimum of 30 years of overlap between standing and LW pairs, t-values were only calculated when the overlap was at least 30 years. All standing trees had chronologies of at least 30 years, but only 2 out of the 10 LW samples met the length requirement. The results for BAI suggest that the LW samples tested possibly came from the near-channel position. Both LW samples had a higher correlation to near-channel trees than upslope trees, with a correlation coefficient of 0.57 and 0.65 for LW-4 and LW-10, respectively (Table 2). These correlations also had significant t values ($t > 3.5$). For RWI, LW-4 (0.53) was correlated highest to a near-channel tree while LW-10 (0.45) correlated highest to an upslope tree, but both correlations were not significant ($t < 3.5$) (Appendix Table A5). With longer chronologies, it is possible that BAI t-values could determine LW source location.

Table 2. Results of t-value matching for basal area increment (BAI).

BAI				
Logjam	**Matched Position**	**Matched Species**	**T-value**	**Correlation (ρ)**
LW-4	Near-Channel	Psme	3.66	0.57

LW-10	Near-Channel	Pien	4.57	0.65

4.6 Comparison of $\delta^{18}O$ Variability by Landscape Position and Species

I expected $\delta^{18}O$ variance to be different between positions and greater in upslope trees because it is assumed upslope trees become more enriched from soil water evaporation. There was no clear separation in $\delta^{18}O$ variance between near-channel and upslope trees for any species. Additionally, the $\delta^{18}O$ variance of LW overlapped both near-channel and upslope trees. There were no significant differences between near-channel and upslope $\delta^{18}O$ variance for ponderosa pine ($p = 0.71$) or Engelmann spruce ($p = 0.90$) (Figure 10a,b). Similar to BAI CV and RWI variance, Douglas-fir could not be tested because of sample size (Figure 10c). This test can't be used with $\delta^{18}O$ to identify the source location of LW. Looking at climate along with $\delta^{18}O$ might be a better indicator of position differences.

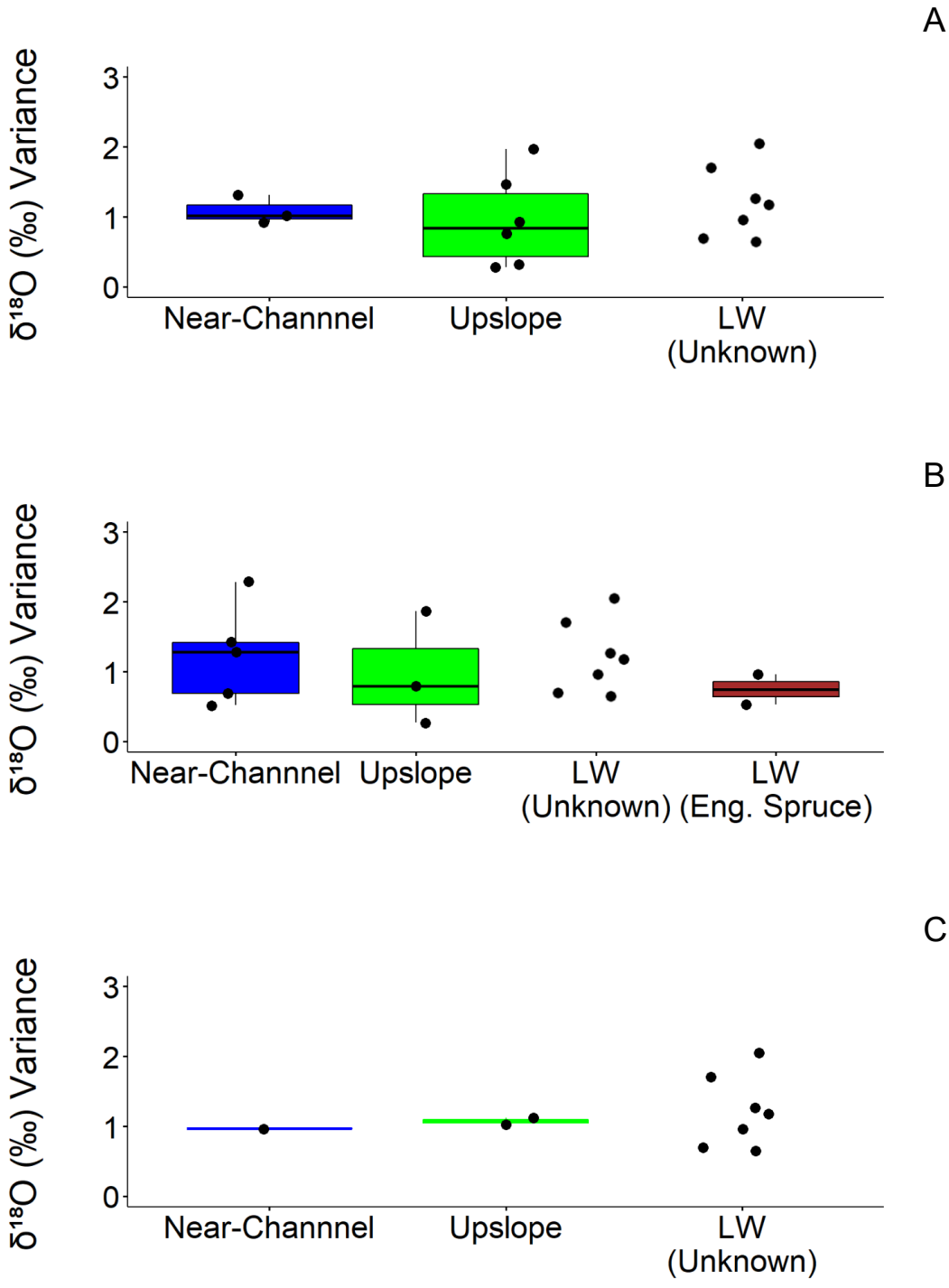

Figure 10. Boxplots of $\delta^{18}O$ variance by position for (A) ponderosa pine, (B) Engelmann spruce, (C) Douglas-fir. Jitter points show the $\delta^{18}O$ variance of each standing tree and LW sample. Large wood (LW) is separated between Engelmann spruce and unknown species.

4.7 Comparison of $\delta^{18}O$ by Landscape Position with Regard to Climate/PDSI

Because $\delta^{18}O$ values are sensitive to drier, more evaporative conditions, I expected that $\delta^{18}O$ values might vary across PDSI categories. Moderate drought, very moist, and extremely moist conditions did not occur in the selected years for analysis of $\delta^{18}O$ (2005-2013). For ponderosa pine, the results of the Kruskal-Wallis test indicated no significant differences in near-channel $\delta^{18}O$ across PDSI categories ($p = 0.42$) or upslope $\delta^{18}O$ across PDSI categories ($p = 0.51$) (Figure 11a). Engelmann spruce also showed no significant differences in near-channel $\delta^{18}O$ across PDSI categories ($p = 0.19$) or upslope $\delta^{18}O$ across PDSI categories ($p = 0.27$) (Figure 11b). Similar to ponderosa pine and Engelmann spruce, Douglas-fir showed no significant differences in near-channel $\delta^{18}O$ ($p = 0.49$) or upslope $\delta^{18}O$ ($p = 0.28$) across PDSI categories (Figure 11c).

Although I did not find differences across PDSI, I thought perhaps trees in the near-channel and upslope positions might differ in $\delta^{18}O$ within drier PDSI categories. Based on the results of the Mann-Whitney U test, there were no significant differences in $\delta^{18}O$ between upslope and near-channel ponderosa pine within any of the PDSI categories ($p > 0.22$ for all comparisons) (Figure 11a). However, there was a significant difference between upslope $\delta^{18}O$ and near-channel $\delta^{18}O$ in Engelmann spruce during mid-range conditions ($p = 0.04$, upslope = 31.4 ‰, near-channel = 30.0 ‰) (Figure 11b, Appendix Figure A12). There were no significant differences between upslope and near-channel Douglas-fir trees ($p > 0.61$) (Figure 11c). There were not enough differences between positions that can be used to identify LW source location.

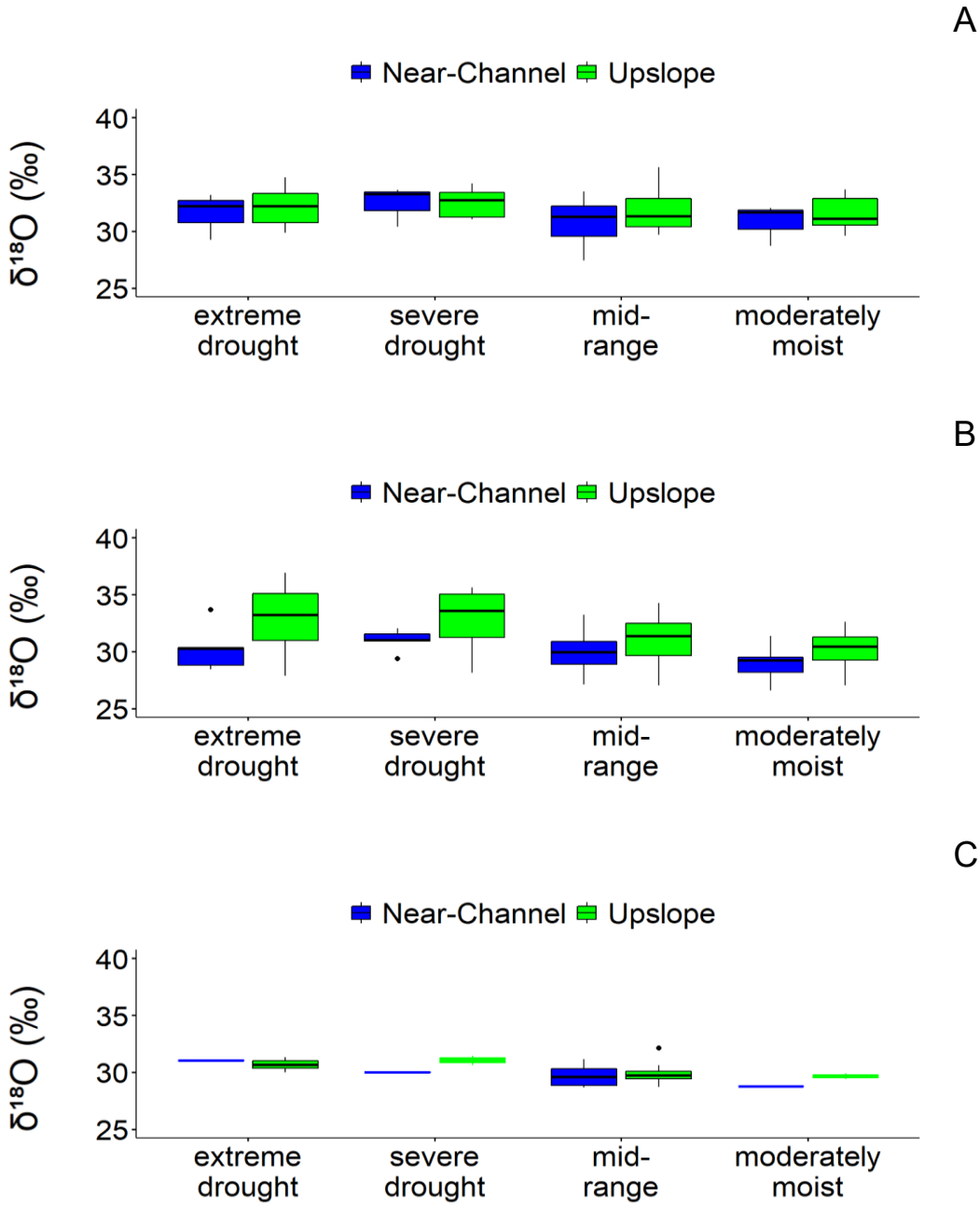

Figure 11. Boxplots of $\delta^{18}O$ by position and PDSI category for (A) ponderosa pine, (B) Engelmann spruce, (C) Douglas-fir.

5. DISCUSSION

5.1 Can dendrochronology metrics (BAI and RWI) be used to identify the source location of LW?

The BAI and RWI time series, variance, and annual growth showed different trends for each species. However, I did not find any indication that BAI and RWI varied enough across the short distances between landscape positions to be used as a tool to source LW. Although other factors in addition to soil moisture can reduce tree growth (e.g., higher VPD, higher temperature, and lower precipitation), I expected lower annual growth and higher growth variability in upslope trees compared to near-channel trees because upslope locations tend to have drier soil during drought conditions, making tree growth more sensitive to local climate (Hewlett and Hibbert, 1963; Vysotskaya and Vaganov, 1989; Teskey and Hinckley, 1986; Blyth, 1999). Any differences found between positions were assumed to come from soil moisture, creating lower growth in upslope trees than near-channel trees under dry conditions, although soil moisture was not directly measured.

Statistical analyses showed no differences in BAI CV between positions or RWI variance between positions (Figure 6). It is interesting that even though Engelmann spruce BAI CV had a significant and positive correlation with elevation along the hillslope (Figure 5b), no differences were found in Engelmann spruce BAI CV between positions. It can be concluded that although Engelmann spruce is increasing in BAI CV along the hillslope, there is not enough separation in BAI CV to show differences between positions or more samples would need to be taken to increase the power of the statistical tests. Because no differences between positions were found, BAI CV and RWI variance could not be used to identify the source location of the LW samples. Calculating the variance and CV using only drought years could show differences in variability

between positions because slight changes in water availability are enhanced during dry years (Vysotskaya and Vaganov, 1989; Teskey and Hinckley, 1986; Schubert, 1974; Adams et al. 2014).

Analysis of the annual BAI of each standing tree sample and the annual PDSI data indicated differences between near-channel and upslope BAI, but only for ponderosa pine (Appendix Figure A8). These results align with the ponderosa pine BAI time series which showed upslope trees having a lower BAI over the full time period and a larger growth decrease during drought years than near-channel trees (Figure 3a). My results are similar to Fuchs et al. (2019) who found ponderosa pine trees growing near-springs in Arizona had higher BAI and were less sensitive to drought than trees farther away from springs. It is unclear why I found differences in annual BAI but not BAI CV. However, it is possible that grouping data by different drought conditions using PDSI can show greater differences in BAI between positions, especially under drier conditions. Additionally, using absolute growth values that indicate year to year variation (annual BAI) could show more differences than relative metrics of dispersion (BAI CV) for a group of years. Adams et al. (2014) used linear mixed effects models to show the effects of annual climate and topography on ponderosa pine growth. Adams et al. (2014) found higher ponderosa pine BAI in areas of higher PDSI and topographic wetness index (TWI). Although my results showed higher ponderosa pine BAI in near-channel trees than upslope trees during extreme PDSI conditions, there was no positional difference in BAI during severe drought conditions (Appendix Figure A8). It is possible that the sample size played a role in these results, because the sample size of upslope ponderosa pine is lowest in severe drought conditions compared to other PDSI categories (Appendix Figure A8). If near-channel tree BAI was higher than upslope trees in extreme, severe, and moderate drought conditions, it could indicate that

annual BAI could be used to identify differences between positions for ponderosa pine trees because dry conditions are when underlying changes in soil moisture are more expressed compared to wet soil conditions (Manrique-Alba et al., 2017). However, my results are mixed.

Similar to BAI CV, Engelmann spruce annual BAI did not show differences between positions (Figure 8b). Based on the time series and boxplots of Engelmann spruce BAI, upslope trees were generally lower in BAI than near-channel trees (Figure 3b, Figure 8b). However, this was not the case when looking at the difference in BAI within PDSI categories. Engelmann spruce has a shallow root system (Alexander, 1987; Burns, 1990) and most roots don't extend more than 46 cm if the trees are growing near the water table (Alexander, 1987). Thus, the lack of difference between positions within PDSI categories was likely not due to deeper roots on the hillslope relative to the near-channel (resulting in similar moisture resources across positions), since Engelmann spruce rooting depths are typically shallow. Based on the BAI results and rooting characteristics, the Engelmann spruce could simply be growing less on the hillslope but not enough to indicate differences in growth between positions.

Douglas-fir also did not have any differences in annual BAI between positions within PDSI categories (Figure 8c). The Douglas-fir time series showed very little difference in near-channel and upslope BAI over the full-time series and during drought years, with exception of 2012 (Figure 3c). Because Douglas-fir roots can extend past 60 cm (Smith, 1964; Burns 1990), they can get their water from deeper soil layers. Looking at the BAI time series and the lack of differences between positions, it is possible that Douglas-fir trees adapted to dry conditions by rooting deeper into the soil than what was originally assumed. Another factor affecting results is sample size. The BAI CV could not be compared between positions because of the low sample size. Although Douglas-fir annual BAI had a larger sample size than BAI CV and could be

compared between positions, the sample size was still small compared to the annual BAI of ponderosa pine and Engelmann spruce (Figure 8c). Without additional sampling, I can't clearly state that Douglas-fir trees are not different between positions.

For all species, there was little significant difference in annual BAI across PDSI categories when looking within near-channel or within upslope trees. Only Douglas-fir responded, with BAI being higher in mid-range conditions compared to extreme drought conditions (Appendix Figure A7). It is unclear why near-channel and upslope BAI were not reacting to climate, especially since the time series of all species showed decreased BAI during drought years compared to non-drought years (Figure 3a-c). As stated before, Douglas-fir had a smaller sample size than ponderosa and Engelmann spruce, with only 2 near-channel trees used for annual BAI. Upslope Douglas-fir may not be reacting during the other PDSI conditions because of the sample size (Appendix Figure A7).

Ponderosa pine RWI did not respond to PDSI and did not meet the expectation that RWI would be different across PDSI conditions (Vysotskaya and Vaganov, 1989; Teskey and Hinckley, 1986). Looking at the time series, ponderosa pine was the least responsive to climate, but still showed RWI decreased in drought years compared to non-drought years when assessing the time series (Figure 3d). Although the time series showed similar trends to that of Adams et al. (2014), who saw reduced RWI in drought years compared to non-drought years, my results were not significant when near-channel and upslope trees were grouped by PDSI categories separately and statistically tested. Adams et al. (2014) also found ponderosa pine RWI was positively correlated to precipitation and negatively correlated to temperature. However, Adams et al. (2014) had sampled some ponderosa pine at a higher elevation (> 2600 m) than all of my study samples (< 2300 m) and had samples separated by a longer distance (> 0.5 km). With

temperature being a limiting factor at higher elevations (Schubert, 1974), Adams et al (2014) was likely able to capture significant climate correlations. The upper elevation limit of ponderosa pine averages 2770 m (Huckaby, 2003), and all of my trees were sampled at an elevation considered best for growth (2100 m - 2400 m) (Schubert, 1974). The small differences in sampling elevation could be the reason why I did not see significant results, because there was not enough moisture stress at my hillslope locations.

The response of annual RWI to PDSI differed by species, with only Engelmann spruce demonstrating a response across PDSI categories (Appendix Figure A9, A10). My time series and statistical analysis both showed upslope and near-channel Engelmann spruce RWI responded to dry climate, decreasing during dry years (Figure 3e). Upslope and near-channel Engelmann spruce showed an increase in RWI in wetter PDSI conditions, indicating both positions respond similarly to regional climate (Appendix Figure A9, A10). The results for annual Engelmann spruce RWI between drought categories align with Truettner et al. (2018) who found Engelmann spruce was decreased in RWI because of high VPD, which was assumed to increase drought conditions for trees. Although Truettner et al. (2018) did not test for RWI differences between positions, the results show a general trend of Engelmann spruce RWI being affected by drought conditions, similar to what I found for both near-channel and upslope Engelmann spruce. Although a general climate response was found, these results can't be used to differentiate between positions.

Similar to Engelmann spruce, Douglas-fir also did not respond to PDSI, even though it had the largest changes in drought years relative to non-drought years when looking at the time series, indicating a possibility that the species would respond to drier climate conditions (Figure 3c). The only response found was a higher upslope RWI during mid-range conditions compared

to extreme drought conditions, similar to what was found for upslope Douglas-fir BAI (Appendix Figure A11). Unlike my results, Carnwath et al. (2012) found Douglas-fir RWI was sensitive to climate and sensitivity was greater at dryer sites. Using linear mixed effects models, Carnwath et al. (2012) found Douglas-fir was more sensitive to PDSI and precipitation in Xeric sites than Dry-Mesic sites. Xeric sites were characterized as having 20% less total precipitation in the summer, an average maximum temperature of 1.5℃ higher, and an average elevation difference of 198.5 m (Xeric = 911m, Dry-Mesic = 1109.5m) compared to Dry-Mesic sites. Carnwath et al. (2012) assumed that differences in Douglas-fir's response to PDSI and precipitation were because of lower water availability in Xeric sites relative to Dry-Mesic sites. Similar to Carnwrath et al. (2012), I expected both near-channel and upslope trees to respond to dry PDSI conditions, but with a larger decrease in upslope trees RWI than near-channel trees because of less local water availability in the upslope position. However, I assumed that soil moisture was a factor of local water availability and not precipitation because there is not enough of an elevation difference for precipitation to change. My study did not show enough climate responses from Douglas-fir near-channel and upslope trees to compare them to LW.

Annual BAI and RWI were used to compare chronologies between LW and standing trees, with the assumption that source location could be identified based on the significance of the correlation (t-values). Results showed no significant correlations among the LW and standing tree chronologies for RWI, but significant correlations were found for the BAI chronologies (Table 2). Only two LW samples could be used for calculating t-values (LW-4 and LW-10), and both had significant positive correlations to near-channel trees (Table 2).

Although my results suggest that 2 out of 10 LW samples may be more similar to the near-channel trees than the upslope trees, further work should likely be completed to test this

method. Longer LW time series are likely necessary to calculate the significance of correlations for all metrics. An overlap of at least 50 years between LW and standing trees would likely provide more accurate t-value results (Gut, 2018; Martin-Benito et al., 2014; Sass-Klaassen et al., 2008). There also has not been a study that correlates tree ring series with LW of unknown species over small distances (e.g., hillslope scale). In addition, tree growth metrics are affected by species, and it is possible that the unknown LW was matched to the incorrect species. Studies using t-value matching often provenance wood of unknown origin if the species or genus is known (Bernabei and Bontadi, 2011; Leland et al., 2021; Kagawa and Leavitt 2010; Bridge, 2012). Although I used t-value matching for wood source location within a single catchment and not for regional provenancing, changes in growth can vary by species over a hillslope (Dymond et al., 2016). Having one dominant species in the study area instead of three or identifying the species of all the sampled LW may improve the use of dendrochronology metrics and isotopes for identifying LW source location. Without addressing the concerns mentioned above, t-value testing would not be helpful in identifying LW source location.

5.2 Can $\delta^{18}O$ metrics be used to identify the source location of LW?

I did not find evidence showing $\delta^{18}O$ variance or annual $\delta^{18}O$ can be used to identify source location. I expected more enriched $\delta^{18}O$ in upslope trees because of evaporative enrichment of ^{18}O in soil water, and less soil moisture in the upslope position causing reductions in transpiration and allowing for relating $\delta^{18}O$ variability to LW source location. Although the average time series showed visual differences in $\delta^{18}O$ between positions, very few statistical differences were found between positions. There were no differences in $\delta^{18}O$ variance between positions (Figure 10a-c). I assumed that upslope trees would get their water from soil layers that are isotopically enriched in $\delta^{18}O$ and upslope trees would vary more in $\delta^{18}O$ because of

increasing evaporation on hillslopes during drier years, while near-channel trees would have less variability because they will have more water access during dry periods (Feldhake and Boyer, 1990; Famiglietti, 1998; Allen et al., 2022). There was no evidence supporting this assumption.

The only difference between positions found was for Engelmann spruce $\delta^{18}O$, with higher upslope $\delta^{18}O$ than near-channel trees during mid-range conditions (Appendix Figure A12). It is unclear why the $\delta^{18}O$ is only different during mid-range conditions, as having different $\delta^{18}O$ during drier PDSI conditions would have provided evidence that upslope and near-channel $\delta^{18}O$ is different because of evaporative enrichment.

It is possible that the soil moisture in my study area was not dry enough to show higher cellulose $\delta^{18}O$. Barnard et al. (2012) found high cellulose $\delta^{18}O$ was related to reduced stomatal conductance. Because stomatal conductance and the Peclet effect is reduced in dry conditions (Lange et al., 1971; Meinzer, 1993; Bond et al., 2008; Barbour, 2007; Farquhar and Lloyd, 1993; Barbour and Farquhar, 2000), higher cellulose $\delta^{18}O$ could be shown if the soil conditions in my study were drier. The rooting depth of my trees could also be playing a role in the results. Rossatto et al. (2012) found that woody savanna plants at higher elevations had more depleted $\delta^{18}O$ than lower elevations. Rossatto et al. (2012) states that higher elevation plants used 70-80% of the top soil layers for water and extracted water from deeper, unsaturated soils compared to lower elevation plants that used 90-100% of the topsoil layer water. I expected the trees I sampled to extract their water from the top soil layers and cause differences in $\delta^{18}O$ because the majority of their roots occur in the upper soil layers (Burns, 1990). I did not expect differences in $\delta^{18}O$ because of uptake from different soil depths. Having deeper roots would mean the trees would get their water from different, more depleted sources than the top soil layers (Depante et al., 2019; Rossatto et al., 2012; Nippert and Knapp, 2007). The rooting depth of my trees could

be deeper than expected, especially for ponderosa pine and Douglas fir, which can have roots past the average depth of Engelmann spruce trees (46 cm) (Schubert, 1974; Smith, 1964; Alexander, 1987). The cellulose itself could also be the reason I did not see $\delta^{18}O$ differences, because further fractionation and exchange during sucrose and cellulose synthesis reduces $\delta^{18}O$ enrichment compared to leaf water $\delta^{18}O$ (Sternberg and DeNiro, 1983; Roden et al., 2000; Barbour, 2007). Although there are caveats to how I measured $\delta^{18}O$ and where I sampled, lack of differences in $\delta^{18}O$ could indicate that there are not enough local evaporation differences between positions to enhance the $\delta^{18}O$ signal. Overall, isotope analysis proved to be ineffective in showing differences between tree positions that could be used for identifying the source location of LW.

5.3 Additional study limitations

Based on the results of BAI, RWI, and $\delta^{18}O$, there was very little evidence supporting these techniques as valid indicators of LW source location. Tree growth and isotope variation metrics were not different between positions and therefore LW could not be easily identified as coming from near the channel or upslope. The hillslope scale in this study was relatively small, with an elevation difference of less than 8 m between near-channel and upslope trees. Increasing the hillslope scale could result in greater differences in soil moisture, affecting tree growth and the isotopic composition of source water. Studies looking at growth and source water between valley bottoms/riparian areas and hillslopes typically characterize trees in positions that differ in elevation by more than 100 m (Mašek et al., 2023; Dudley et al., 2018). But the ability to expand the scale is based on the study site.

Aspect could also be affecting my results because aspect affects tree growth (Mašek et al., 2023; Fekedulegn et al. 2003; Kelsey et al. 2018). Mašek et al. (2023) found differences in

tree ring width along a topographic gradient and on hillslopes with differing aspects, with trees in upslope positions and on south-facing slopes having smaller tree ring widths. Fekedulegn et al. (2003) also found dry slopes exhibit lower growth rates in yellow-polar, red oak, and red maple. Kelsey et al. (2018) found a decline in subalpine fir growth on east- and south-facing slopes. In my study, trees were sampled on both north-facing and south-facing slopes, but I did not separate them during analysis because the sample size was already small. Sampling more trees and separating them by aspect could highlight growth changes because of differences in sun exposure that affect soil moisture (McAneney and Noble, 1976; Swift and Knoerr, 1973; Garnier and Ohmura, 1970; Hinckley et al., 2014).

This study aimed to assess whether there are differences between standing tree growth and $\delta^{18}O$ between near-channel and hillslope positions to identify the source location of LW. Testing new techniques for wood sourcing includes not only determining which tree species to use but also which metric may provide better differences in growing conditions to compare against LW. However, the results of my study indicate that more work would be needed to determine the conditions under which tree growth metrics and isotopes would provide insight into source location

6. CONCLUSION

There are currently few methods for studying the spatial source of LW. My study attempted to assess new potential techniques for LW sourcing (e.g., near-channel or hillslope) within a single catchment by using dendrochronology and isotopes. Differences in BAI, RWI, and $\delta^{18}O$ by position were assessed for three species growing in the upper montane/subalpine zone of the Colorado Front Range. The metrics are meant to indicate differences in growth and evaporation along hillslope because of inferred local soil moisture differences. There was very little evidence suggesting dendrochronology or isotopes can be used to determine the source location of LW. Due to the importance of LW in river corridors, constraining wood budgets through identifying LW source locations and the proportion of LW coming from different portions of the landscape is important. The methods presented in this study introduce new techniques for LW wood source, with the hope that other studies improve the methodology for future wood budget estimates.

REFERENCES

Adams, H. R., Barnard, H. R., & Loomis, A. K. (2014). Topography alters tree growth–climate relationships in a semi-arid forested catchment. *Ecosphere*, *5*(11), 1-16.

Alexander, R. R. (1987). *Ecology, silviculture, and management of the Engelmann spruce-subalpine fir type in the central and southern Rocky Mountains* (No. 659). US Department of Agriculture, Forest Service.

Allen, S. T., Sprenger, M., Bowen, G. J., & Brooks, J. R. (2022). Spatial and Temporal Variations in Plant Source Water: O and H Isotope Ratios from Precipitation to Xylem Water. In *Stable Isotopes in Tree Rings: Inferring Physiological, Climatic and Environmental Responses* (pp. 501-535). Cham: Springer International Publishing.

Baillie, M. G. (2014). *Tree-ring dating and archaeology*. Routledge.

Barbour, M. M. (2007). Stable oxygen isotope composition of plant tissue: a review. *Functional Plant Biology*, 34(2), 83-94.

Barbour, M. M., & Farquhar, G. D. (2000). Relative humidity-and ABA-induced variation in carbon and oxygen isotope ratios of cotton leaves. *Plant, Cell & Environment*, 23(5), 473-485.

Barnard, H. R., Brooks, J. R., & Bond, B. J. (2012). Applying the dual-isotope conceptual model to interpret physiological trends under uncontrolled conditions. *Tree physiology*, 32(10), 1183-1198.

Benda, L. E., Bigelow, P., & Worsley, T. M. (2002). Recruitment of wood to streams in old-growth and second-growth redwood forests, northern California, USA. *Canadian Journal of Forest Research*, 32(8), 1460-1477.

Benda, L. E., & Sias, J. C. (2003). A quantitative framework for evaluating the mass balance of in-stream organic debris. *Forest ecology and management*, 172(1), 1-16.

Beria, H., Larsen, J. R., Ceperley, N. C., Michelon, A., Vennemann, T., & Schaefli, B. (2018). Understanding snow hydrological processes through the lens of stable water isotopes. *Wiley Interdisciplinary Reviews: Water*, 5(6), e1311.

Bernabei, M., & Bontadi, J. (2011). Determining the resonance wood provenance of stringed instruments from the Cherubini Conservatory Collection in Florence, Italy. *Journal of cultural heritage*, 12(2), 196-204.

Bigeleisen, J. (1962). Correlation of tritium and deuterium isotope effects. *In Tritium in the Physical and Biological Sciences. V. 1. Proceedings of a Symposium*.

Blyth, E. M. (1999). Estimating potential evaporation over a hill. *Boundary-layer meteorology*,

92(2), 185-193.

Bond, B. J., Meinzer, F. C., & Brooks, J. R. (2008). How trees influence the hydrological cycle in forest ecosystems. *Hydroecology and ecohydrology: Past, present and future*, 7-28.

Boswijk, G., & Fowler, A. M. (2019). Dendroprovenancing: a preliminary assessment of potential to geo-locate kauri timbers in northern New Zealand. *Dendrochronologia*, 57, 125611.

Bridge, M. (2012). Locating the origins of wood resources: a review of dendroprovenancing. *Journal of Archaeological Science*, 39(8), 2828-2834.

Buffington, J. M., Montgomery, D. R., & Greenberg, H. M. (2004). Basin-scale availability of salmonid spawning gravel as influenced by channel type and hydraulic roughness in mountain catchments. *Canadian Journal of Fisheries and Aquatic Sciences*, 61(11), 2085-2096.

Buhay, W. M., & Edwards, T. W. (1995). Climate in southwestern Ontario, Canada, between AD 1610 and 1885 inferred from oxygen and hydrogen isotopic measurements of wood cellulose from trees in different hydrologic settings. *Quaternary Research*, 44(3), 438-446.

Bunn A, Korpela M, Biondi F, Campelo F, Mérian P, Qeadan F, Zang C (2022). *_dplR: Dendrochronology Program Library in R_*. R package version 1.7.4, <https://CRAN.R-project.org/package=dplR>.

Burk, R. L., & Stuiver, M. (1981). Oxygen isotope ratios in trees reflect mean annual temperature and humidity. *Science*, 211(4489), 1417-1419.

Burns, R. M. (1990). *Silvics of North America: Conifers* (No. 654). US Department of Agriculture, Forest Service.

Caldwell, M. (1985). Cold desert. Physiological ecology of North American plant communities, 198-212.Carnwath, G. C., Peterson, D. W., & Nelson, C. R. (2012). Effect of crown class and habitat type on climate–growth relationships of ponderosa pine and Douglas-fir. *Forest Ecology and Management*, 285, 44-52.

Cernusak, L. A., Wong, S. C., & Farquhar, G. D. (2003). Oxygen isotope composition of phloem sap in relation to leaf water in Ricinus communis. *Functional Plant Biology*, 30(10), 1059-1070.

Chimner, R. A., & Cooper, D. J. (2004). Using stable oxygen isotopes to quantify the water source used for transpiration by native shrubs in the San Luis Valley, Colorado USA. *Plant and Soil*, 260, 225-236.

Clark, I. D., & Fritz, P. (1997). *Environmental isotopes in hydrogeology*. CRC press.

Cook, E. R. (1985). *A time series analysis approach to tree ring standardization* (Doctoral dissertation, University of Arizona).

Cook, E. R., & Peters, K. (1981). The smoothing spline: a new approach to standardizing forest interior tree-ring width series for dendroclimatic studies. *Tree-ring Bulletin*.

Cooper, J. D., Gardner, C. M. K., & Mackenzie, N. (1990). Soil controls on recharge to aquifers. *Journal of Soil Science*, 41(4), 613-630.

Craig, H., and L. I. Gordon (1965), Deuterium and oxygen 18 variations in the ocean and the marine atmosphere, in *Stable Isotopes in Oceanographic Studies and Paleotemperatures*, edited by E. Tongiorgi, pp. 9 –130, Lab. Geol. Nucl., Pisa, Italy.

Cuntz, M., Ogée, J., Farquhar, G. D., Peylin, P., & Cernusak, L. A. (2007). Modeling advection and diffusion of water isotopologues in leaves. *Plant, Cell & Environment*, 30(8), 892-909.

Dansgaard, W. (1954). The O18-abundance in fresh water. *Geochimica et Cosmochimica Acta*, 6(5-6), 241-260.

Dawson, T. E. (1993). Water sources of plants as determined from xylem-water isotopic composition: perspectives on plant competition, distribution, and water relations. In *Stable isotopes and plant carbon-water relations* (pp. 465-496). Academic Press.

Dawson, T. E., & Ehleringer, J. R. (1991). Streamside trees that do not use stream water. *Nature*, 350(6316), 335-337.

Dawson, T. E., & Pate, J. S. (1996). Seasonal water uptake and movement in root systems of Australian phraeatophytic plants of dimorphic root morphology: a stable isotope investigation. *Oecologia*, 107, 13-20.

DeNiro, M. J., & Epstein, S. (1981). Isotopic composition of cellulose from aquatic organisms. *Geochimica et Cosmochimica Acta*, 45(10), 1885-1894.

Depante, M., Morison, M. Q., Petrone, R. M., Devito, K. J., Kettridge, N., & Waddington, J. M. (2019). Hydraulic redistribution and hydrological controls on aspen transpiration and establishment in peatlands following wildfire. *Hydrological Processes*, 33(21), 2714-2728.

Dongmann, G., Nürnberg, H. W., Förstel, H., & Wagener, K. (1974). On the enrichment of H218O in the leaves of transpiring plants. *Radiation and environmental biophysics*, 11(1), 41-52.

Dudley, B. D., Marttila, H., Graham, S. L., Evison, R., & Srinivasan, M. S. (2018). Water

sources for woody shrubs on hillslopes: An investigation using isotopic and sapflow methods. *Ecohydrology*, 11(2), e1926.

Dymond, S. F., D'Amato, A. W., Kolka, R. K., Bolstad, P. V., Sebestyen, S. D., & Bradford, J. B. (2016). Growth–climate relationships across topographic gradients in the northern Great Lakes. *Ecohydrology*, 9(6), 918-929.

Epstein, S., Thompson, P., & Yapp, C. J. (1977). Oxygen and hydrogen isotopic ratios in plant cellulose. *Science*, 198(4323), 1209-1215.

Famiglietti, J. S., Rudnicki, J. W., & Rodell, M. (1998). Variability in surface moisture content along a hillslope transect: Rattlesnake Hill, Texas. *Journal of hydrology*, 210(1-4), 259-281.

Farquhar, G. D., & Lloyd, J. (1993). Carbon and oxygen isotope effects in the exchange of carbon dioxide between terrestrial plants and the atmosphere. In *Stable isotopes and plant carbon-water relations* (pp. 47-70). Academic Press.

Fekedulegn, D., Hicks Jr, R. R., & Colbert, J. J. (2003). Influence of topographic aspect, precipitation and drought on radial growth of four major tree species in an Appalachian watershed. *Forest ecology and management*, 177(1-3), 409-425.

Feldhake, C. M., & Boyer, D. G. (1990). Bellani evaporation variation in hill-land pasture. *Agricultural and forest meteorology*, 51(3-4), 211-222.

Fritts, H. C. (1966). Growth-Rings of Trees: Their Correlation with Climate: Patterns of ring widths in trees in semiarid sites depend on climate-controlled physiological factors. *Science*, 154(3752), 973-979.

Fuchs, L., Stevens, L. E., & Fulé, P. Z. (2019). Dendrochronological assessment of springs effects on ponderosa pine growth, Arizona, USA. *Forest Ecology and Management*, 435, 89-96.

Garnier, B. J., & Ohmura, A. (1970). The evaluation of surface variations in solar radiation income. *Solar energy*, 13(1), 21-34.

Gazis, C., & Feng, X. (2004). A stable isotope study of soil water: evidence for mixing and preferential flow paths. *Geoderma*, 119(1-2), 97-111.

Gerhard, M., & Reich, M. (2000). Restoration of streams with large wood: effects of accumulated and built-in wood on channel morphology, habitat diversity and aquatic fauna. *International Review of Hydrobiology: A Journal Covering all Aspects of Limnology and Marine Biology*, 85(1), 123-137.

Gessler, A., Ferrio, J. P., Hommel, R., Treydte, K., Werner, R. A., & Monson, R. K. (2014).

Stable isotopes in tree rings: towards a mechanistic understanding of isotope fractionation and mixing processes from the leaves to the wood. *Tree physiology*, 34(8), 796-818.

Gochis, D., Schumacher, R., Friedrich, K., Doesken, N., Kelsch, M., Sun, J., ... & Brown, B. (2015). The Great Colorado Flood of September 2013, *Bulletin of the American Meteorological Society*, 96(9), 1461-1487.

Gonfiantini, R. (1984). IAEA advisory group meeting on stable isotope reference samples for geochemical and hydrological investigations. *Chemical geology*, 46(1), 85.

Guiney, M. R., & Lininger, K. B. (2022). Disturbance and valley confinement: Controls on floodplain large wood and organic matter jam deposition in the Colorado Front Range, USA. *Earth Surface Processes and Landforms*, 47(6), 1371-1389.

Gut, U. (2018). Evaluating the key assumptions underlying dendro-provenancing: How to spruce it up with a scissor plot. *Dendrochronologia*, 52, 131-145.

Haneca, K., Wazny, T., Van Acker, J., & Beeckman, H. (2005). Provenancing Baltic timber from art historical objects: success and limitations. *Journal of archaeological Science*, 32(2), 261-271.

Harvey, F. E. (2005). Stable hydrogen and oxygen isotope composition of precipitation in Northeastern Colorado. *JAWRA Journal of the American Water Resources Association*, 41(2), 447-460.

Harvey, J., & Gooseff, M. (2015). River corridor science: Hydrologic exchange and ecological consequences from bedforms to basins. *Water Resources Research*, 51(9), 6893-6922.

Heddinghaus, T. R., & Sabol, P. (1991). A review of the Palmer Drought Severity Index and where do we go from here. In *Proc. 7th Conf. on Applied Climatology* (pp. 242-246). Boston, MA, USA: American Meteorological Society.

Heim Jr, R. R. (2002). A review of twentieth-century drought indices used in the United States. *Bulletin of the American Meteorological Society*, 83(8), 1149-1166.

Hewlett, J. D., & Hibbert, A. R. (1963). Moisture and energy conditions within a sloping soil mass during drainage. *Journal of geophysical research*, 68(4), 1081-1087.

Hilton, S. (2012). Large woody debris budgets in the Caspar Creek Experimental Watersheds. *In Redwood Forests in a Changing California Science Symposium* (p. 51).

Hinckley, E. L. S., Ebel, B. A., Barnes, R. T., Anderson, R. S., Williams, M. W., & Anderson, S. P. (2014). Aspect control of water movement on hillslopes near the rain–snow transition of the Colorado Front Range. *Hydrological Processes*, 28(1), 74-85.

Hornbeck, J. W., & Smith, R. B. (1985). Documentation of red spruce growth decline. *Canadian*

Journal of Forest Research, 15(6), 1199-1201.

Hosty, M., & Mulqueen, J. (1996). Soil moisture and groundwater drawdown in a dry grassland soil. *Irish journal of agricultural and food research*, 17-24.

Huckaby, L. S. (2003). *Field guide to old ponderosa pines in the Colorado Front Range*. United States Department of Agriculture, Forest Service, Rocky Mountain Research Station.

Jacobson, P. J., Jacobson, K. M., Angermeier, P. L., & Cherry, D. S. (1999). Transport, retention, and ecological significance of woody debris within a large ephemeral river. *Journal of the North American Benthological Society*, 18(4), 429-444.

Kagawa, A., & Leavitt, S. W. (2010). Stable carbon isotopes of tree rings as a tool to pinpoint the geographic origin of timber. *Journal of Wood Science*, 56(3), 175-183.

Kelsey, K. C., Redmond, M. D., Barger, N. N., & Neff, J. C. (2018). Species, climate and landscape physiography drive variable growth trends in subalpine forests. *Ecosystems*, 21, 125-140.

Keys, T. A., Govenor, H., Jones, C. N., Hession, W. C., Hester, E. T., & Scott, D. T. (2018). Effects of large wood on floodplain connectivity in a headwater Mid-Atlantic stream. *Ecological Engineering*, 118, 134-142.

Lange, O. L., Lösch, R., Schulze, E. D., & Kappen, L. (1971). Responses of stomata to changes in humidity. *Planta*, 100, 76-86.

Leavitt, S. W., & Danzer, S. R. (1993). Method for batch processing small wood samples to holocellulose for stable-carbon isotope analysis. *Analytical Chemistry*, 65(1), 87-89.

Leland, C., Rao, M. P., Cook, E. R., Cook, B. I., Lapidus, B. M., Staniforth, A. B., ... & Rodriguez-Caton, M. (2021). Dendroarchaeological analysis of the Terminal Warehouse in New York City reveals a history of long-distance timber transport during the Gilded Age. *Journal of Archaeological Science: Reports*, 39, 103114.

Li, J., Chen, F., Cook, E. R., Gou, X., & Zhang, Y. (2007). Drought reconstruction for north central China from tree rings: the value of the Palmer drought severity index. International *Journal of Climatology: A Journal of the Royal Meteorological Society*, 27(7), 903-909.

Lininger, K. B., & Hilton, S. (2022). Large Wood in Small Channels: A 20-Year Study of Budgets and Piece Mobility in Two Redwood Streams. *Water Resources Research*, 58(11).

Lininger, K. B., Scamardo, J. E., & Guiney, M. R. (2021). Floodplain large wood and organic

matter jam formation after a large flood: Investigating the influence of floodplain forest stand characteristics and river corridor morphology. *Journal of Geophysical Research: Earth Surface*, 126(6).

Lininger, K. B., Wohl, E., Sutfin, N. A., & Rose, J. R. (2017). Floodplain downed wood volumes: a comparison across three biomes. *Earth Surface Processes and Landforms*, 42(8), 1248–1261.

MacVicar, B. J., Piégay, H., Henderson, A., Comiti, F., Oberlin, C., & Pecorari, E. (2009). Quantifying the temporal dynamics of wood in large rivers: field trials of wood surveying, dating, tracking, and monitoring techniques. *Earth Surface Processes and Landforms*, 34(15), 2031-2046.

Manrique-Alba, À., Ruiz-Yanetti, S., Moutahir, H., Novak, K., De Luis, M., & Bellot, J. (2017). Soil moisture and its role in growth-climate relationships across an aridity gradient in semiarid Pinus halepensis forests. *Science of the Total Environment*, 574, 982-990.

Marigo, G., Peltier, J. P., Girel, J., & Pautou, G. (2000). Success in the demographic expansion of Fraxinus excelsior L. Trees, 15, 1-13. Martin, D. J., & Benda, L. E. (2001). Patterns of instream wood recruitment and transport at the watershed scale. *Transactions of the American Fisheries Society*, 130(5), 940-958.

Martin, D. J., Pavlowsky, R. T., Bendix, J., Dogwiler, T., & Hess, J. (2023). Impacts of an extreme flood on large wood recruitment and transport processes. *Physical Geography*, 44(1), 55-83.

Martin-Benito, D., Pederson, N., McDonald, M., Krusic, P., Fernandez, J. M., Buckley, B., ... & Cook, E. (2014). Dendrochronological dating of the world trade center ship, lower Manhattan, New York City. *Tree-ring research*, 70(2), 65-77.

Mašek, J., Tumajer, J., Lange, J., Kaczka, R., Fišer, P., & Treml, V. (2023). Variability in Tree-ring Width and NDVI Responses to Climate at a Landscape Level. *Ecosystems*, 1-14.

McDade, M. H., Swanson, F. J., McKee, W. A., Franklin, J. F., & Sickle, J. V. (1990). Source distances for coarse woody debris entering small streams in western Oregon and Washington. *Canadian Journal of Forest Research*, 20(3), 326-330.

McAneney, K. J., & Noble, P. F. (1976). Estimating solar radiation on sloping surfaces. *New Zealand journal of experimental agriculture*, 4(2), 195-202.

Meinzer, F. C. (1993). Stomatal control of transpiration. *Trends in Ecology & Evolution*, 8(8), 289-294.

Merten, E. C., Vaz, P. G., Decker-Fritz, J. A., Finlay, J. C., & Stefan, H. G. (2013). Relative importance of breakage and decay as processes depleting large wood from streams. *Geomorphology*, 190, 40-47.

Milton, M. J., & Wielgosz, R. I. (2002). Use of the international system of units (SI) in isotope ratio mass spectrometry. *Rapid communications in mass spectrometry*, 16(23), 2201-2204.

Nakamura, F., Swanson, F. J., & Wondzell, S. M. (2000). Disturbance regimes of stream and riparian systems—a disturbance-cascade perspective. *Hydrological Processes*, 14(16-17), 2849-2860.

Nippert, J. B., & Knapp, A. K. (2007). Linking water uptake with rooting patterns in grassland species. *Oecologia*, 153, 261-272.

Palmer, W.C., (1965). *Meteorological drought*. Research Paper No. 45. U.S. Weather Bureau. NOAA Library and Information Services Division, Washington, D.C. 20852.

Penna, D., Geris, J., Hopp, L., & Scandellari, F. (2020). Water sources for root water uptake: Using stable isotopes of hydrogen and oxygen as a research tool in agricultural and agroforestry systems. *Agriculture, Ecosystems & Environment*, 291, 106790.

Peterken, G. F., & Mountford, E. P. (1996). Effects of drought on beech in Lady Park Wood, an unmanaged mixed deciduous woodland. *Forestry: An International Journal of Forest Research*, 69(2), 125-136.

Piegay, H., & Gurnell, A. M. (1997). Large woody debris and river geomorphological pattern: examples from SE France and S. England. *Geomorphology*, 19(1-2), 99-116.

Piégay, H., Moulin, B., & Hupp, C. R. (2017). Assessment of transfer patterns and origins of in-channel wood in large rivers using repeated field surveys and wood characterization (the Isère River upstream of Pontcharra, France). *Geomorphology*, 279, 27-43.

Piégay, H., Thévenet, A., & Citterio, A. (1999). Input, storage and distribution of large woody debris along a mountain river continuum, the Drôme River, France. *Catena*, 35(1), 19-39.

Poca, M., Coomans, O., Urcelay, C., Zeballos, S. R., Bodé, S., & Boeckx, P. (2019). Isotope fractionation during root water uptake by Acacia caven is enhanced by arbuscular mycorrhizas. *Plant and Soil*, 441, 485-497.

PRISM Climate Group, Oregon State University, https://prism.oregonstate.edu/explorer/, data created June 2013, revised December 2022.

Rathburn, S. L., Bennett, G. L., Wohl, E. E., Briles, C., McElroy, B., & Sutfin, N. (2017). The fate of sediment, wood, and organic carbon eroded during an extreme flood, Colorado Front Range, USA. *Geology*, 45(6), 499-502.

R Core Team (2022). *R: A language and environment for statistical computing*. R Foundation for Statistical Computing, Vienna, Austria. URL https://www.R-project.org/.

Reeves, G. H., Burnett, K. M., & McGarry, E. V. (2003). Sources of large wood in the main stem of a fourth-order watershed in coastal Oregon. *Canadian Journal of Forest Research*, 33(8), 1363-1370.

Reid, D. A., & Hassan, M. A. (2020). Response of in-stream wood to riparian timber harvesting: Field observations and long-term projections. *Water Resources Research*, 56(8), e2020WR027077.

Roden, J. S., Lin, G., & Ehleringer, J. R. (2000). A mechanistic model for interpretation of hydrogen and oxygen isotope ratios in tree-ring cellulose. *Geochimica et Cosmochimica Acta*, 64(1), 21-35.

Rossatto, D. R., Silva, L. D. C. R., Villalobos-Vega, R., Sternberg, L. D. S. L., & Franco, A. C. (2012). Depth of water uptake in woody plants relates to groundwater level and vegetation structure along a topographic gradient in a neotropical savanna. *Environmental and Experimental Botany*, 77, 259-266.

Ruiz-Villanueva, V., Mazzorana, B., Bladé, E., Bürkli, L., Iribarren-Anacona, P., Mao, L., … & Wohl, E. (2019). Characterization of wood-laden flows in rivers. *Earth Surface Processes and Landforms*, 44(9), 1694-1709.

Russell, M. B., Fraver, S., Aakala, T., Gove, J. H., Woodall, C. W., D'Amato, A. W., & Ducey, M. J. (2015). Quantifying carbon stores and decomposition in dead wood: A review. *Forest Ecology and Management*, 350, 107-128.

Sargeant, C. I., Singer, M. B., & Vallet-Coulomb, C. (2019). Identification of source-water oxygen isotopes in trees toolkit (ISO-Tool) for deciphering historical water use by forest trees. *Water Resources Research*, 55(12), 10954-10975.

Sass-Klaassen, U., Vernimmen, T., & Baittinger, C. (2008). Dendrochronological dating and provenancing of timber used as foundation piles under historic buildings in The Netherlands. *International Biodeterioration & Biodegradation*, 61(1), 96-105.

Saurer, M., Robertson, I., Siegwolf, R., & Leuenberger, M. (1998). Oxygen isotope analysis of cellulose: an interlaboratory comparison. *Analytical Chemistry*, 70(10), 2074-2080.

Schubert, G. H. (1974). *Silviculture of southwestern ponderosa pine: the status of our knowledge* (Vol. 123). Rocky Mountain Forest and Range Experiment Station, Forest Service, US Department of Agriculture.

Scott, D. N., & Wohl, E. (2020). Geomorphology and climate interact to control organic carbon stock and age in mountain river valley bottoms. *Earth Surface Processes and Landforms*, 45(9), 1911-1925.

Sheppard, J. C., & Funk, W. H. (1975). Trees as environmental sensors monitoring long-term

heavy metal contamination of Spokane River, Idaho. *Environmental Science & Technology*, 9(7), 638-642.

Sheshshayee, M. S., Bindumadhava, H., Ramesh, R., Prasad, T. G., Lakshminarayana, M. R., & Udayakumar, M. (2005). Oxygen isotope enrichment (Δ18O) as a measure of time-averaged transpiration rate. *Journal of Experimental Botany*, 56(422), 3033-3039.

Siegwolf, R. T., Brooks, J. R., Roden, J., & Saurer, M. (2022). *Stable isotopes in tree rings: inferring physiological, climatic and environmental responses*. Springer Nature.

Smith, J. H. G. (1964). Root spread can be estimated from crown width of Douglas fir, lodgepole pine, and other British Columbia tree species. *The Forestry Chronicle*, 40(4), 456-473.

Song, X., Lorrey, A., & Barbour, M. M. (2022). Environmental, physiological and biochemical processes determining the oxygen isotope ratio of tree-ring cellulose. *In Stable Isotopes in Tree Rings: Inferring Physiological, Climatic and Environmental Responses* (pp. 311-329). Cham: Springer International Publishing.

Sternberg, L., & DeNiro, M. J. D. (1983). Biogeochemical implications of the isotopic equilibrium fractionation factor between the oxygen atoms of acetone and water. *Geochimica et Cosmochimica Acta*, 47(12), 2271-2274.

Sternberg, L., Pinzon, M. C., Anderson, W. T., & Jahren, A. H. (2006). Variation in oxygen isotope fractionation during cellulose synthesis: intramolecular and biosynthetic effects. *Plant, Cell & Environment*, 29(10), 1881-1889.

Sutfin, N. A., Wohl, E. E., & Dwire, K. A. (2016). Banking carbon: a review of organic carbon storage and physical factors influencing retention in floodplains and riparian ecosystems. *Earth Surface Processes and Landforms*, 41(1), 38-60.

Swift, L. W., & Knoerr, K. R. (1973). Estimating solar radiation on mountain slopes. *Agricultural Meteorology*, 12, 329-336.

Tang, K., & Feng, X. (2001). The effect of soil hydrology on the oxygen and hydrogen isotopic compositions of plants' source water. *Earth and Planetary Science Letters*, 185(3-4), 355-367.

Teskey, R. O., & Hinckley, T. M. (1986). Moisture: effects of water stress on trees. In *Stress physiology and forest productivity: Proceedings of the Physiology Working Group Technical Session*. Society of American Foresters National Convention, Fort Collins, Colorado, USA, July 28–31, 1985 (pp. 9-33). Springer Netherlands.

Truettner, C., Anderegg, W. R., Biondi, F., Koch, G. W., Ogle, K., Schwalm, C., ... & Ziaco, E. (2018). Conifer radial growth response to recent seasonal warming and drought from the southwestern USA. *Forest ecology and management*, 418, 55-62.

Tuzet, A., Perrier, A., & Leuning, R. (2003). A coupled model of stomatal conductance, photosynthesis and transpiration. *Plant, Cell & Environment*, 26(7), 1097-1116.

Urey, H. C. (1947). The thermodynamic properties of isotopic substances. *Journal of the Chemical Society* (Resumed), 562-581.

Urey, H. C. (1948). Oxygen isotopes in nature and in the laboratory. Science, 108(2810), 489-496. Vargas, A. I., Schaffer, B., Yuhong, L., & Sternberg, L. D. S. L. (2017). Testing plant use of mobile vs immobile soil water sources using stable isotope experiments. *New Phytologist*, 215(2), 582-594.

Vega-Grau, A. M., McDonnell, J., Schmidt, S., Annandale, M., & Herbohn, J. (2021). Isotopic fractionation from deep roots to tall shoots: a forensic analysis of xylem water isotope composition in mature tropical savanna trees. *Science of the Total Environment*, 795, 148675.

Vysotskaya, L. G., & Vaganov, E. A. (1989). Components of the variability of radial cell size in tree rings of conifers. *IAWA Journal*, 10(4), 417-426.

Warren, D. R., & Kraft, C. E. (2008). Dynamics of large wood in an eastern US mountain stream. *Forest Ecology and Management*, 256(4), 808-814.

Weigl, M. (2006). *Annual and intra-annual variations of ring-widths and stable isotopes in sessile oak (Quercus petraea (Matt.) Liebl.)* (Thesis, Universität für Bodenkultur Wien).

Wershaw, R. L., Friedman, I. R. V. I. N. G., Heller, S. J., & Frank, P. A. (1966). Hydrogen isotopic fractionation of water passing through trees. *Advanced in Organic Geochemistry*, 55-67.

Wohl, E. (2017). Bridging the gaps: An overview of wood across time and space in diverse rivers. *Geomorphology*, 279, 3-26.

Wohl, E., Kramer, N., Ruiz-Villanueva, V., Scott, D. N., Comiti, F., Gurnell, A. M., ... & Fausch, K. D. (2019). The natural wood regime in rivers. *BioScience*, 69(4), 259-273.

Wondzell, S. M., LaNier, J., Haggerty, R., Woodsmith, R. D., & Edwards, R. T. (2009). Changes in hyporheic exchange flow following experimental wood removal in a small, low-gradient stream. *Water Resources Research*, 45(5).

Yanosky, T. M., & Vroblesky, D. A. (1992). Relation of nickel concentrations in tree rings to groundwater contamination. *Water Resources Research*, 28(8), 2077-2083.

Yochum, S. E., & Moore, D. S. (2013). *Colorado Front Range flood of 2013: Peak flow estimates at selected mountain stream locations*. USDA Natural Resources Conservation Service Tech. Rep, 44.

Zimmermann, U., Ehhalt, D., & Münnich, K. O. (1968). *Soil-water movement and evapotranspiration: changes in the isotopic composition of the water*. The University of Heidelberg.

APPENDIX A

Table A1. Standing tree data including species, reach, hillslope position, and tree elevation difference from stream (vertical distance). Ponderosa pine (Pipo), Douglas-fir (Psme), Engelmann spruce (Pien).

Tree ID	Species	Reach	Elevation from Stream (m)
LW-1	Unknown	34	0.4
LW-2	Pien	34	0.1
LW-3	Unknown	34	-0.1
LW-4	Unknown	34	0
LW-5	Pien	28	0.4
LW-6	Unknown	28	-0.2
LW-7	Unknown	28	2
LW-8	Unknown	28	2
LW-9	Unknown	28	2
LW-10	Unknown	28	1.2

Table A2. Minimum and maximum values for large wood (LW) basal area increment (BAI), ring width index (RWI), and $\delta^{18}O$.

Logjam	Minimum BAI (mm^2)	Maximum BAI (mm^2)	Minimum RWI	Maximum RWI	Minimum $\delta^{18}O$ (‰)	Maximum $\delta^{18}O$ (‰)
LW-1	567.33	1962.90	0.58	1.33	28.96	30.84
LW-2	352.90	662.56	0.68	1.20	29.07	32.48
LW-3	883.40	1614.08	0.77	1.12	27.87	30.67

LW-4	147.02	643.23	0.43	1.97	30.19	33.05
LW-5	393.13	1348.80	0.72	1.26	32.28	34.54
LW-6	1177.64	3082.89	0.61	1.26	28.08	30.70
LW-7	99.14	1171.18	0.50	1.49	30.97	36.61
LW-8	906.51	1632.42	0.77	1.25	27.24	30.54
LW-9	347.29	666.58	0.75	1.33	28.43	32.67
LW-10	873.79	2055.37	0.76	1.20	27.05	31.08

Table A3. Large wood ring width index (RWI) and $\delta^{18}O$ during drought years.

Logjam	RWI 2002	RWI 2006	RWI 2012	$\delta^{18}O$ 2006	$\delta^{18}O$ 2012
LW-1	1.29	0.82	1.12	30.30	30.84
LW-2	0.86	0.68	0.88	30.62	31.34
LW-3	1.01	0.90	1.10	28.93	28.62
LW-4	0.72	1.13	0.67	32.64	30.31
LW-5	0.72	0.94	0.95	33.82	34.54
LW-6	0.98	0.61	0.70	30.36	29.85

LW-7	0.75	1.01	0.93	36.61	32.94
LW-8	0.77	0.83	0.98	29.17	30.54
LW-9	1.13	0.80	0.95	32.68	30.63
LW-10	0.98	0.92	0.99	31.08	29.92

Table A4. Results of t-value matching for basal area increment (BAI). Matched position and matched species are based on the highest t-value and highest correlation coefficient within the large wood (LW) and standing tree pair.

BAI

Logjam	Matched Position	Matched Species	T-value	Correlation (ρ)
LW-1	Upslope	Pien	-	0.36
LW-2	Upslope	Pien	-	0.27
LW-3	Near-Channel	Psme	-	0.49
LW-4	Near-Channel	Psme	3.66	0.57
LW-5	Upslope	Pien	-	0.50
LW-6	Near-Channel	Pien	-	0.74
LW-7	Upslope	Pien	-	0.79
LW-8	Near-Channel	Pien	-	0.81

LW-9	Near-Channel	Pipo	-	0.38
LW-10	Near-Channel	Pien	4.57	0.65

Table A5. Results of t-value matching for ring width index (RWI). Matched position and matched species are based on the highest t-value and highest correlation coefficient within the large wood (LW) and standing tree pair.

RWI

Logjam	Matched Position	Matched Species	T-value	Correlation (ρ)
LW-1	Near-Channel	Pien	-	0.39
LW-2	Upslope	Pien	-	0.49
LW-3	Upslope	Pien	-	0.42
LW-4	Near-Channel	Pien	3.33	0.53
LW-5	Upslope	Pien	-	0.57
LW-6	Upslope	Psme	-	0.85
LW-7	Upslope	Pien	-	0.69
LW-8	Upslope	Pien	-	0.64
LW-9	Near-Channel	Pien	-	0.47

LW-10	Upslope	Psme	2.70	0.45

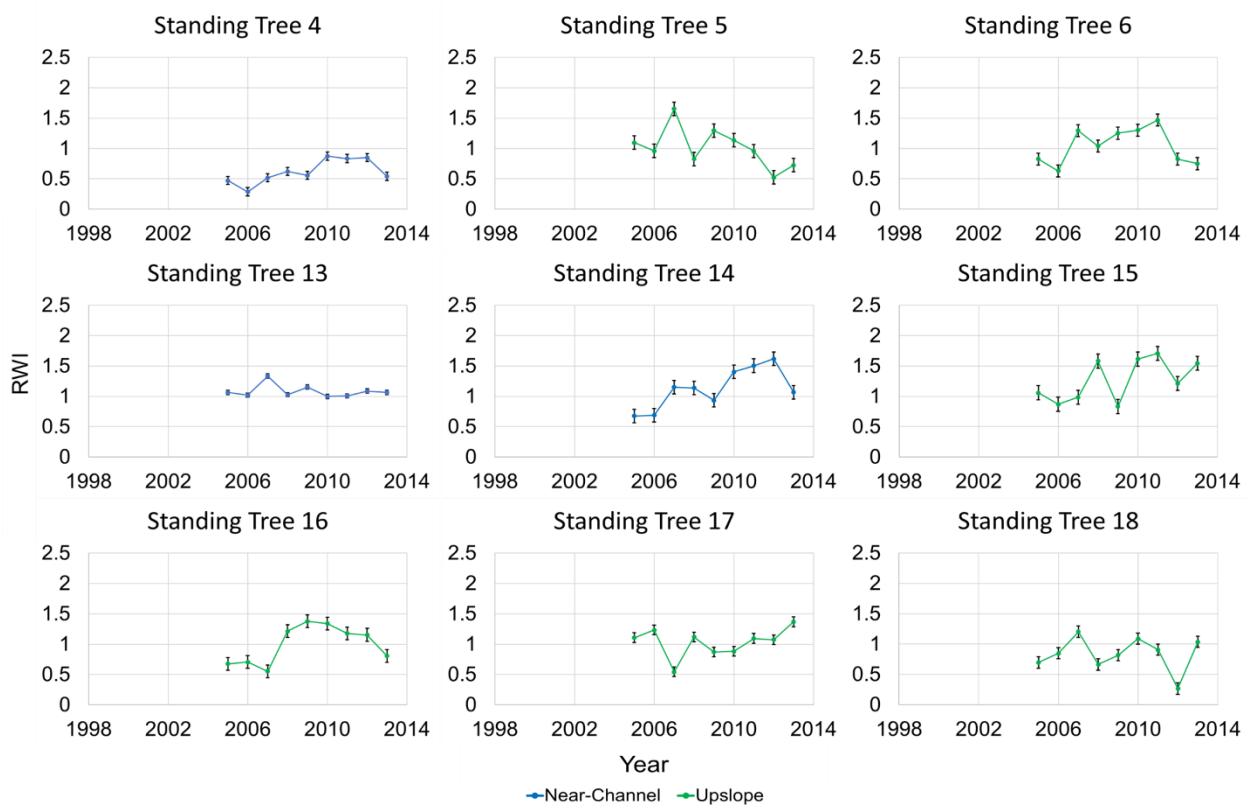

Figure A1. RWI time series of individual ponderosa pine trees.

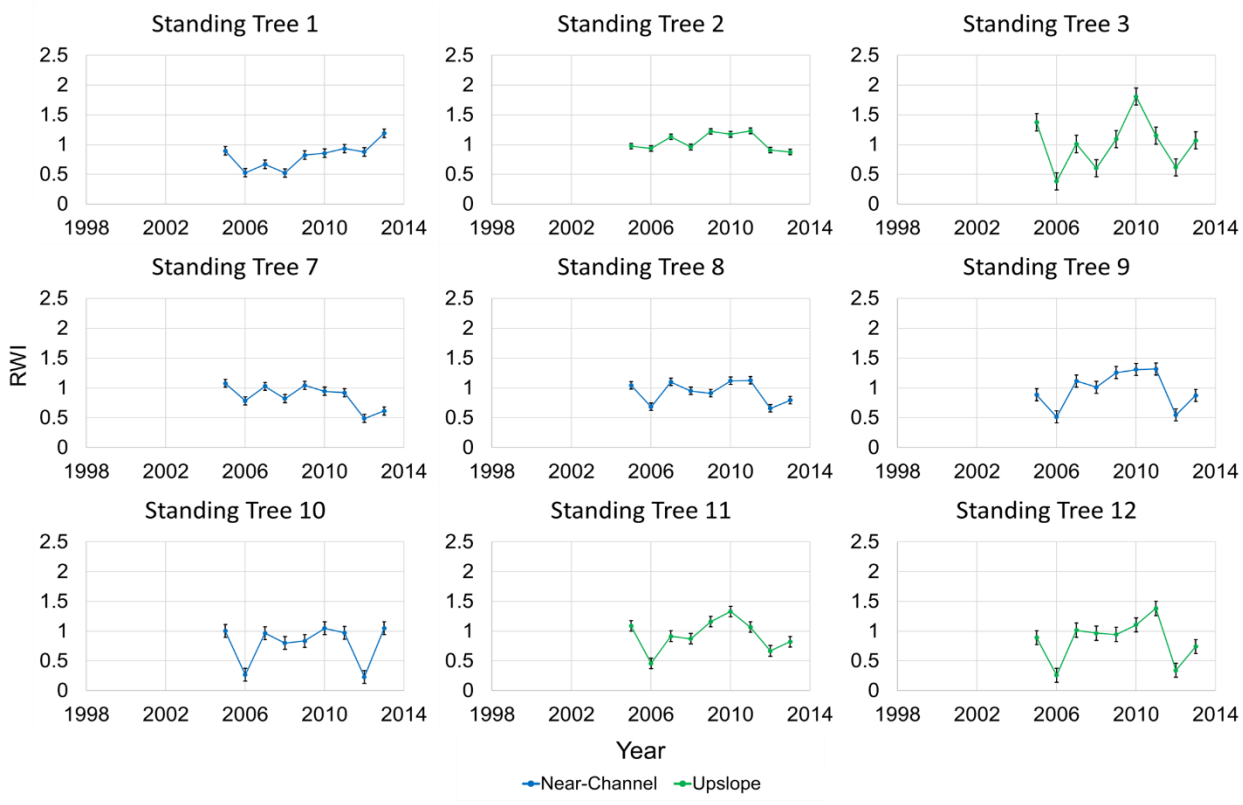

Figure A2. RWI time series of individual Engelmann spruce trees.

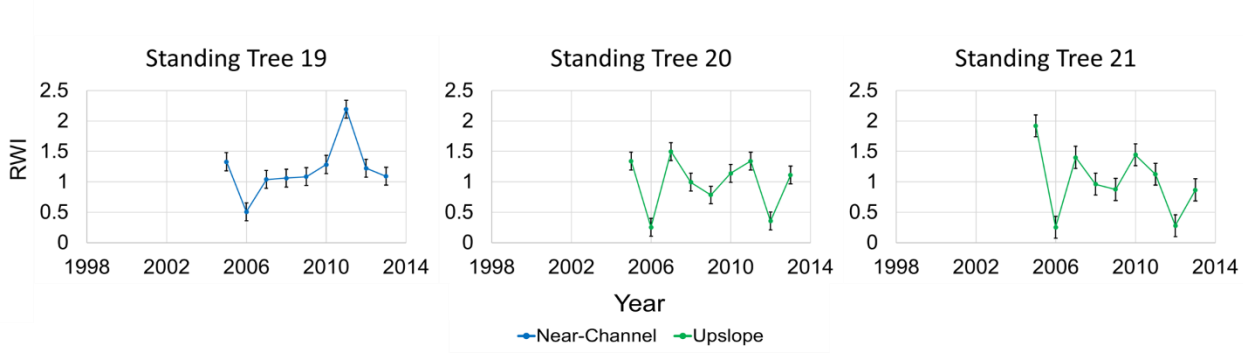

Figure A3. RWI time series of individual Douglas-fir trees.

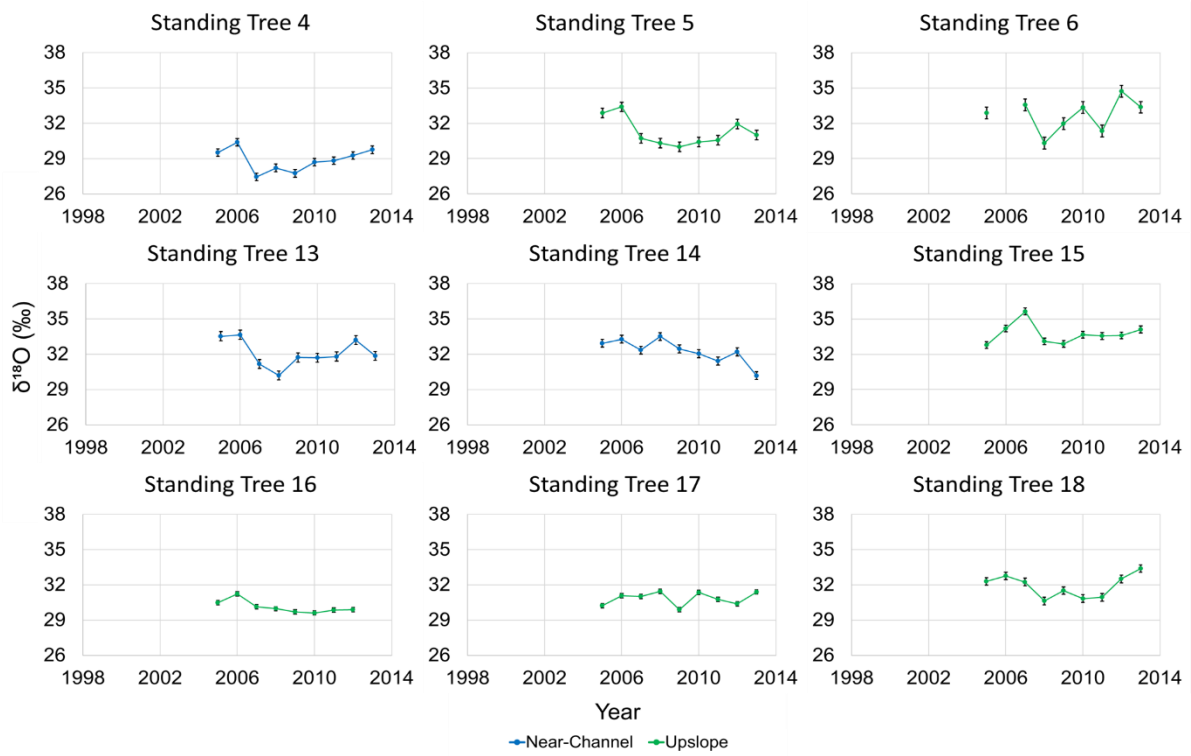

Figure A4. $\delta^{18}O$ time series of individual ponderosa pine trees. Blank sections between 1999-2013 indicate missing data.

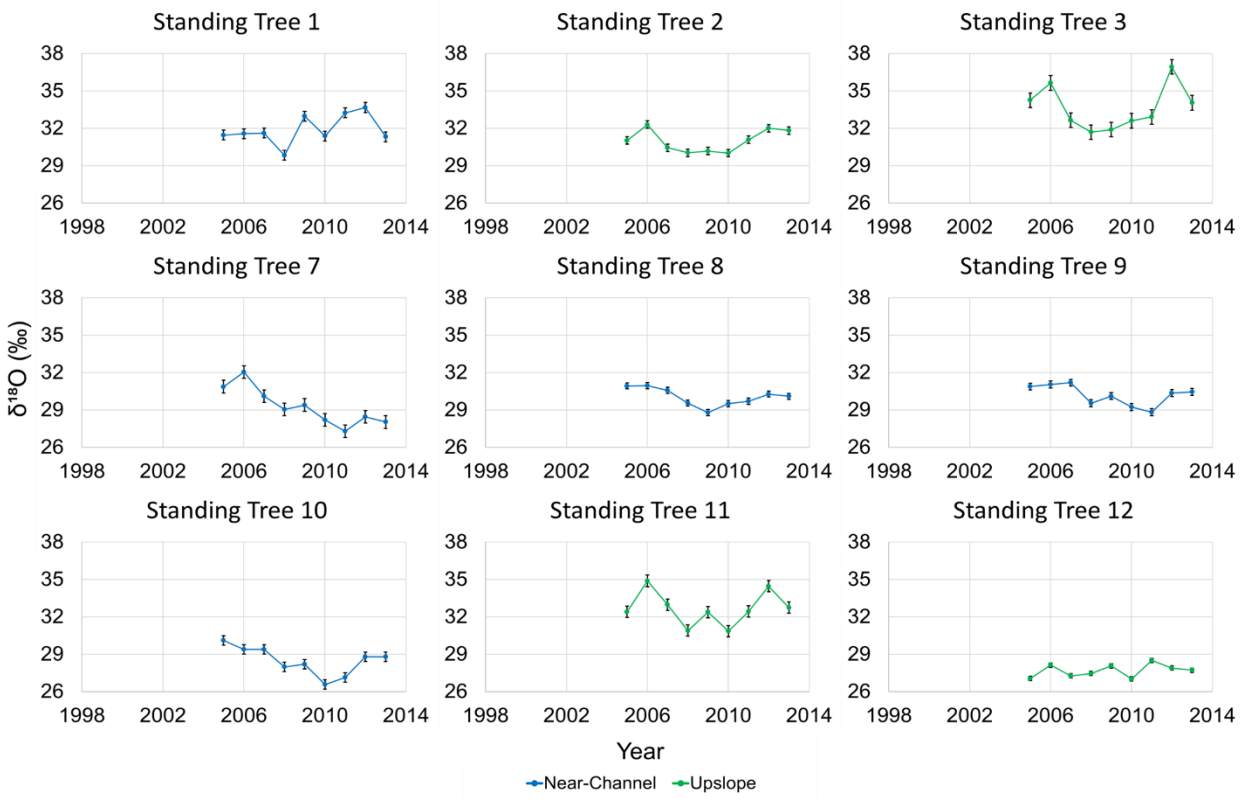

Figure A5. $\delta^{18}O$ time series of individual Engelmann spruce trees.

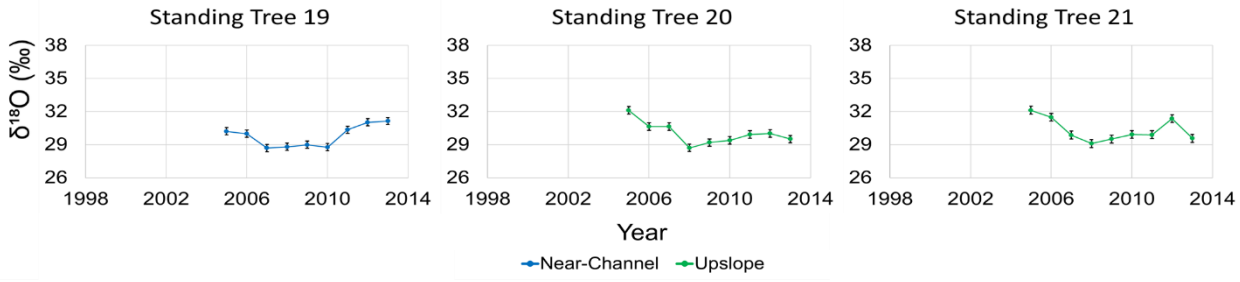

Figure A6. $\delta^{18}O$ time series of individual Douglas-fir trees

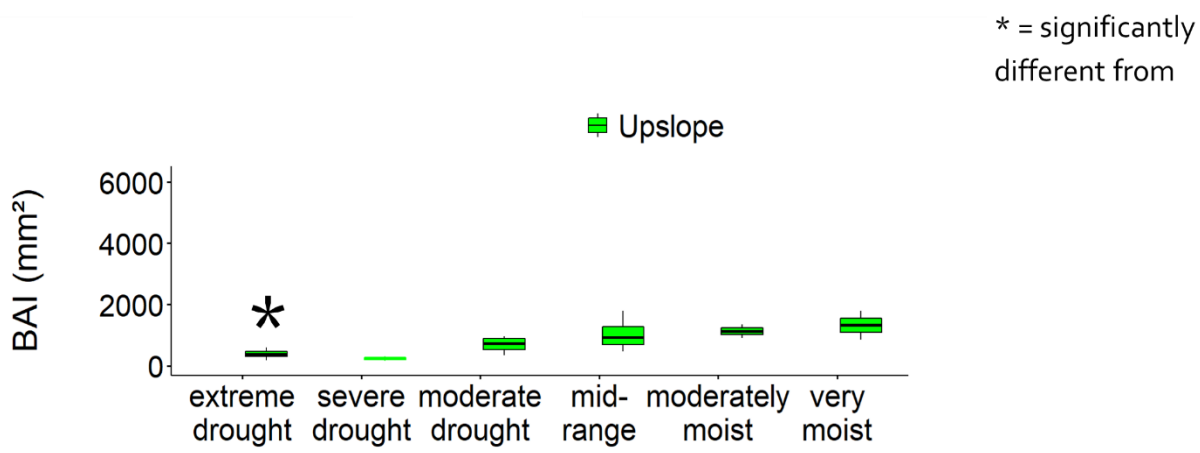

Figure A7. Differences in BAI across PDSI categories for upslope Douglas-fir

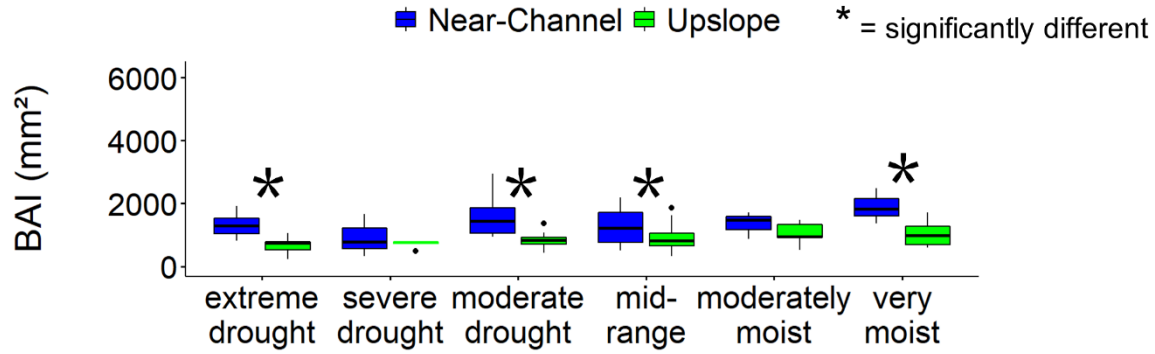

Figure A8. Differences in BAI between positions for ponderosa pine.

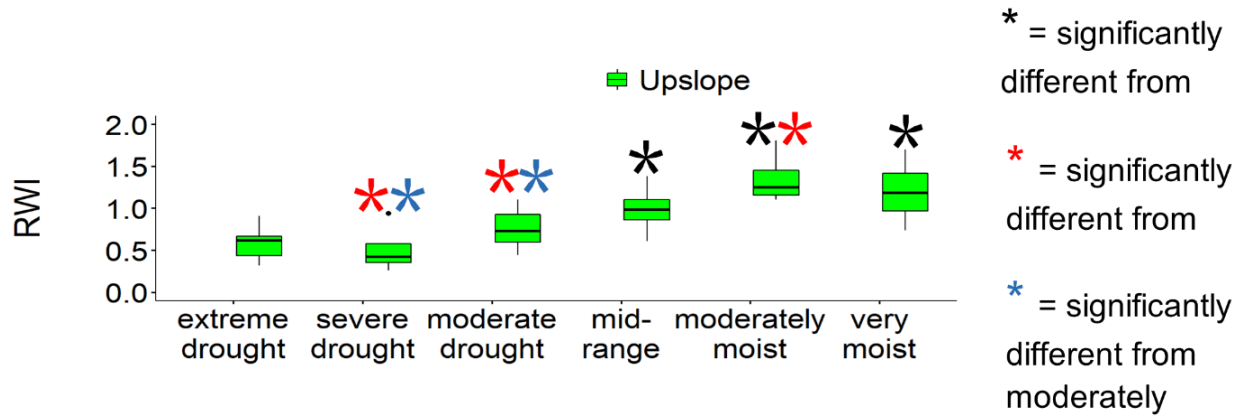

Figure A9. Differences in RWI across PDSI categories for upslope Engelmann spruce.

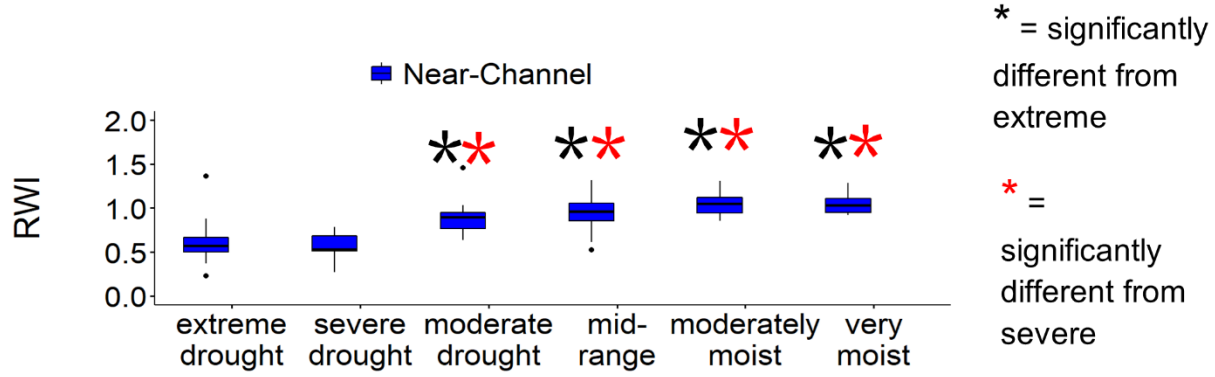

Figure A10. Differences in RWI across PDSI categories for near-channel Engelmann spruce.

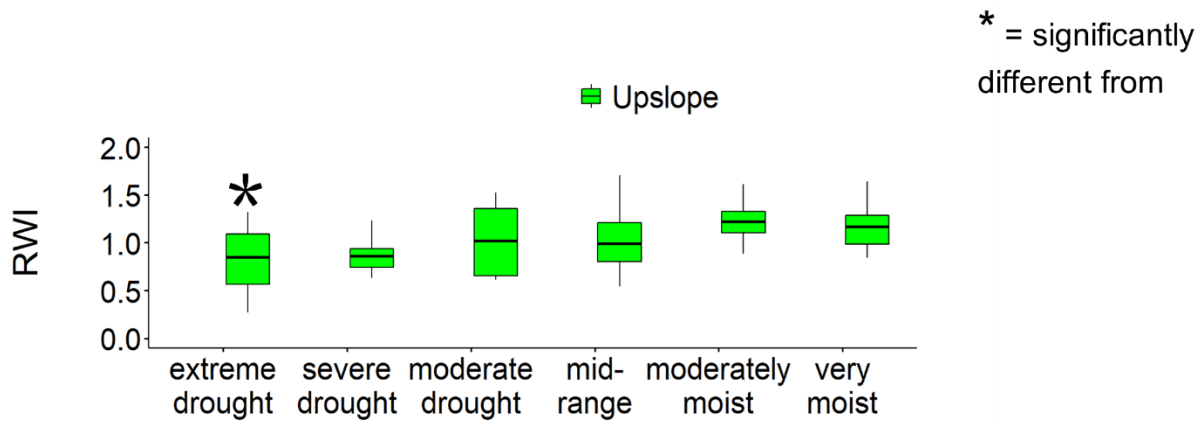

Figure A11. Differences in RWI across PDSI categories for upslope Douglas-fir.

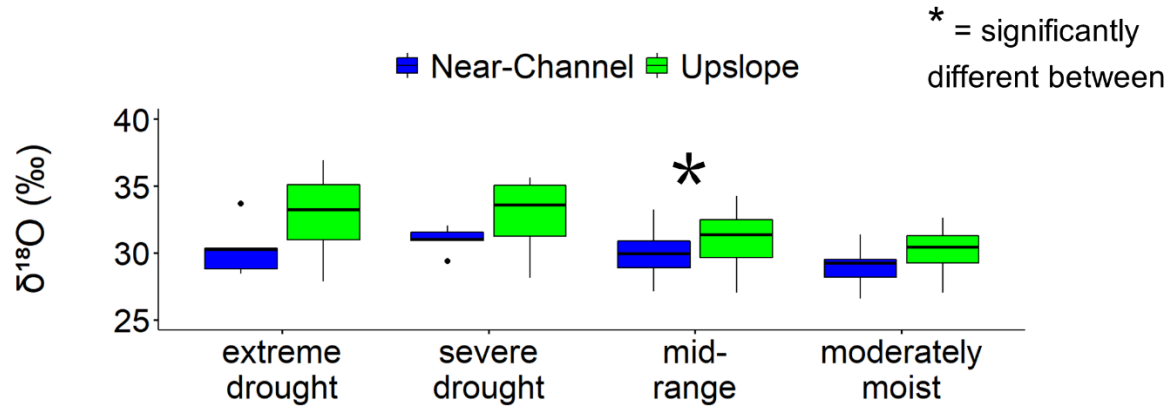

Figure A12. Differences in $\delta^{18}O$ between positions for Engelmann spruce.